ISSN-1560-604X
Thermology international

Thermology International

Volume 29 (2019)
Number 4 (November)

Methods of Scoring the TISEM-Checklist with an Example of Application?

The reliability of an Achilles tendon infrared image analysis method

A case study on dynamic thermal imaging evaluation of a thyroid nodule

This journal is indexed in
EMBASE/Scopus

Published by the
European Association of Thermology

THERMOLOGY INTERNATIONAL

Volume 29 (2019) **Number 4 (November)**

Published by the
European Association of Thermology

Indexed in
Embase/Scopus

Organ of the American Academy of Thermology
Organ of the Brazilian Society of Thermology
Organ of the European Association of Thermology
Organ of the Polish Society of Thermology

Contents

Original article

Kurt Ammer
Methods of Scoring the TISEM-Checklist with an Example of Application.....127
(Methoden zur Scorewertbildung bei der TISEM-Checkliste mit einem Anwendungsbeispiel)

Ben Oliver, A. Munro. S.M. Gerald, L.C. Herrington
The reliability of an Achilles tendon infrared image analysis method. 136
(Die Zuverlässigkeit einer Methode zur Analyse von Infrarot-Wärmebildern der Achillessehne)

Ricardo Vardasca, C. Magalhaes. C. Freitas, J. Mendes
A case study on dynamic thermal imaging evaluation of a thyroid nodule.....146
(Eine Fallstudie zur Auswertung eines dynamischen Wärmebildes eines Schilddrüsenknotens)

News in Thermology

Wroclaw announced as host city for the
XV Congress of the European Association of Thermology, 1st – 4th September 2021.....154

Meetings

Meeting calendar.....156

Methods of Scoring the TISEM-Checklist with an example of application

Kurt Ammer

European Association of Thermology, Vienna, Austria
Faculty of Computing, Engineering and Science, University of South Wales, Pontypridd, United Kingdom

SUMMARY

BACKGROUND: The TISEM-checklist was used as a quality assessment tool of studies reporting infrared imaging studies, but the best method for scoring is yet unclear.

OBJECTIVE: To compare 3 methods of scoring and to investigate whether articles that cite the TISEM achieve higher scores than articles that do not cite the checklist.

METHOD: Database were searched for articles that cite the TISEM. Clinical studies were extracted from the found hits and evaluated using two versions of an ordinal scale and a quantitative scale. An identified review article used an ordinal scale for quality assessment of 33 articles. All clinical studies that cited the TISEM and all articles, already scored in the review article, were evaluated by the three scoring methods. Two groups of articles were built, articles that quoted the TISEM and articles that did not cite the checklist and their scores were compared using the Mann-Witney-test. Agreement of scores in the review article and of the repeated scoring was evaluated by Bland-Altman-plots.

RESULTS. The quantitative scoring performed best in quantifying incomplete reporting. Agreement of the repeated scoring with the original ordinal score was fair with wide limits of agreement (22 points). TISEM citing articles showed significantly higher scores (70% completeness of reporting) than papers that did not quote the TISEM (40% completeness of reporting).

CONCLUSION: Awareness of the checklist may be an effective strategy for improving complete reporting of thermal imaging studies. However, quality assessment of clinical thermography studies should not be restricted to the application of the TISEM checklist.

KEYWORDS: quality assessment, thermal imaging studies, TISEM, infrared thermography

METHODEN ZUR SCOREWERTBILDUNG BEI DER TISEM-CHECKLISTE MIT EINEM ANWENDUNGSBEISPIEL

HINTERGRUND: Die TISEM-Checkliste wurde als Instrument für Qualitätsbewertung von Studien mit Infrarot-Thermographie eingesetzt, jedoch ist die beste Methode für die Bewertung noch unklar.

ZIELSETZUNG: 3 Methoden der Bewertung zu vergleichen und zu untersuchen, ob Artikel, die die TISEM zitieren, höhere Punktzahlen erzielen als Artikel, welche die Checkliste nicht zitieren.

METHODE: Die Datenbank wurde nach Artikeln durchsucht, die die TISEM zitieren. Klinische Studien wurden aus den gefundenen Treffern extrahiert und mit einem 2 Ordinal-Skalen und einer quantitativen Skala ausgewertet. In einem identifizierten Review-Artikel wurde bereits eine der ordinalen Skalen für die Qualitätsbewertung von 33 Artikeln verwendet. Alle klinischen Studien, die die TISEM zitierten, und alle Artikel, die bereits im Review-Artikel bewertet worden waren, wurden nach den drei Methoden der Score-Bildung bewertet. Es wurden zwei Gruppen von Artikeln gebildet: Artikel, die die TISEM zitierten, und Artikel, die die Checkliste nicht zitierten, und ihre Score-Werte wurden mit dem Mann-Witney-Test verglichen. Die Übereinstimmung der Scores im Übersichtsartikel mit den Ergebnissen der wiederholten Bewertung wurde mit Bland-Altman-Plots untersucht.

ERGEBNISSE. Die quantitative Bewertungsmethode schnitt bei der Quantifizierung einer unvollständigen Berichterstattung am besten ab. Die Übereinstimmung der wiederholten Score-Bestimmung mit dem ursprünglichen ordinalem Score-Wert war akzeptabel, bot aber weite Zustimmungsgrenzen (22 Punkte). TISEM zitierende Artikel zeigte deutlich höhere Werte (70% Vollständigkeit der Berichterstattung) als Arbeiten, welche die TISEM nicht zitierten (40% Vollständigkeit der Berichterstattung).

SCHLUSSFOLGERUNG: Die Kenntnis die Checkliste kann eine wirksames Strategie zur Verbesserung der vollständigen Berichterstattung bei Wärmebildstudien sein. Die Qualitätsbewertung klinischer Thermographie-Studien sollte sich jedoch nicht auf die Anwendung der TISEM-Checkliste beschränken.

SCHLÜSSELWÖRTER: Qualitätsbewertung, Wärmebildstudien, TISEM, Infrarot-Thermographie

Thermology international 2019, 29(4) 127-135

Introduction

The Thermal Imaging in Sports and Exercise Medicine (TISEM) Checklist [1] was developed in a Delphi process between 2016- 2017 aiming a consensus on reporting thermographic studies in sports and exercise medicine as authors stated in [2]. Meanwhile, more than 40 articles have cited the TISEM, most of them referenced the checklist as guideline for designing their own thermographic study, but two papers applied the checklist as a tool for quality control by checking the complete reporting of conditions, that cause uncertainties in temperature measurements derived from infrared thermal images.

The checklist includes 15 items in 5 domains such as subject conditions, ambient conditions, camera conditions, image capture and image analysis [3]. Their reporting is classified as absent, unclear or complete. When used for quality control, different methods of scoring are found in the literature. Vardasca et al. scored an absent reporting as zero points, unclear reporting with 1 point and complete reporting with 2 points, resulting in a possible maximal score of 30 points [4]. In a previous pilot study [4], complete reporting scored 3 points, incomplete or unclear information received 2 points, and missing information was labelled with 1 point. Scoring an item with 3 points followed the principle, that an absent condition must be exclusively reported as absent to be labelled as completely reported item. Lack of information on subitems resulted in a score of 2 points. The need of an alternative approach to scoring was discussed due to the fact, that the class of unclear reporting is inhomogeneous, because some items of the TISEM are composed of different numbers of sub-items. Irrespective of the number of missing sub-items, incomplete reporting was always scored with 2 points.

The original aim of this study was to identify articles citing the TISEM article [1] extracting clinical studies from the citations and apply the TISEM to check complete reporting in the articles. Since the search identified a review article [4] that applied the checklist as a tool for quality assessment, the study aim was modified. The extended study goal is a comparison of complete reporting in articles, that have been scored in [4], with identified clinical papers, that cited the TISEM. For evaluation 3 different methods of scoring will be used.

Methods

Data selection

The databases Google Scholar, Web of Science (WoS), Scopus were searched for the TISEM article [1] and the number of citing articles was recorded. The identified citing articles were classified as review article or report of a clinical study and all detected clinical studies were considered for scoring by the TISEM checklist. These articles have been assigned to the TISEM quoting group.

One systematic review [4] had used the TISEM checklist as a tool for quality assessment of included articles and scored thereby 33 articles These articles form the not quoting group. Finally, full versions of all these articles were retrieved, which was not successful in 3 papers. The search strategy and number of hits are presented in Figure 1

Figure 1
Search strategy

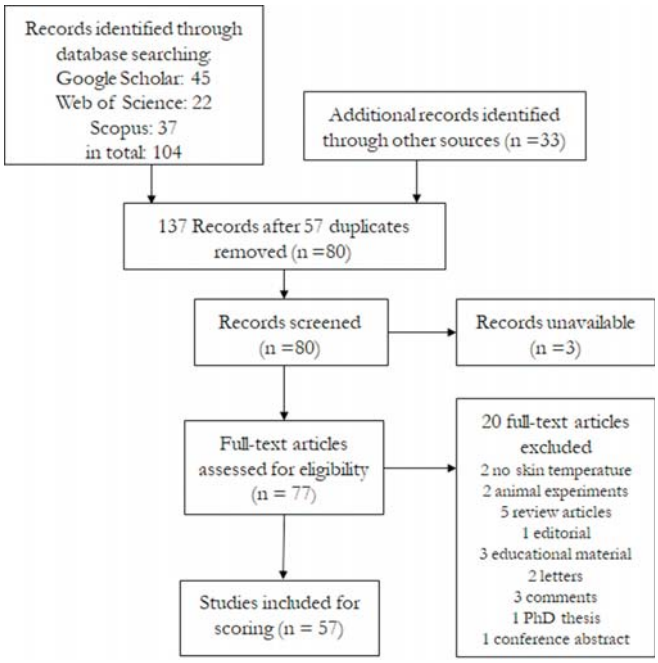

Article assessment and scoring

The scores from [4] were copied. In this article [4] an absent reporting scored zero points, unclear reporting 1 point and complete reporting 2 points, resulting in a possible maximal score of 30 points. It remains unclear, whether scoring was performed consensual by all or some authors or reflect the opinion of single author only.

In the current study, the author assessed all included articles using the TISEM. The following three methods of scoring were applied.

Ordinal scale 1 (OS1) [5]

The original nominal scale of the TISEM may also be understood as ranking, like an ordinal scale from nil to maximum possible. Since item 14 (method of drying wet skin) may not applicable, which scores zero points, a scale from 1 (=absent) over 2 (=incomplete or unclear reporting) to 3 (=complete reporting) seems appropriate. Consequently, the minimal sum score is equal to the number of applicable items, and the maximal score is the 3-fold minimal score. The corresponding mean of the minimal score is equal to 1 point, and the highest possible mean of the maximal score is 3 points.

Ordinal scale 2 (OS2) [4]

An ordinal scale from 0 to 2 allows semi-quantification of the completeness of reporting. However, a zero score is not unambiguous, because it may represent absence of reporting or lack of applicability. The range of sum scores is between 0 and 30, the corresponding mean values are between 0 and 2.

Table 1
Frequencies of reporting per item comparing articles that quoted the TISEM checklist with articles that did not cite.

	Quoting articles (n=25)				Non quoting articles (n=32)			
	Complete reporting (% of cases)	Incomplete reporting (% of cases)	No reporting (% of cases)	Not applicable	Complete reporting (% of cases)	incomplete reporting (% of cases)	No reporting (% of cases)	Not applicable
Item 1	88	12	0		62.5	31.25	6.25	
Item 2	54.17	20.83	25	1	18.74	3.13	78.13	
Item 3	37.5	25	37.5	1	15.62	9.38	75	
Item 4	56	32	12		21.88	56.24	21.88	
Item 5	48	24	28		12.5	15.62	71.88	
Item 6	80	20	0		53.13	43.74	3.13	
Item 7	72	28	24		65.63	3.13	31.24	
Item 8	36	4	60		3.13	3.13	93.74	
Item 9	68	28	4		21.88	53.12	25.00	
Item 10	52	28	20		18.74	28.13	53.13	
Item 11	60	4	36		34.38		65.62	
Item 12	52	12	36		12.5	3.13	84.37	
Item 13	60	20	20		25	48.87	28.13	
Item 14	57.14	14.29	28.57	18	100			30
Item 15	87.5	12.5	0		37.5	53.13	9.37	

Quantitative Scale (QS)

A continuous scale from 0 (=absent reporting) to 1 (=complete reporting) may be used to estimate the quantity of complete reporting. Since some items are composed of subitems, the original defines a class of unclear or incomplete reporting. Unclear reporting is scored with an estimate of 0.5 points. Reporting of subitems is scored proportionally, for example, in case of 4 subitems each receives 0.25 points. Range of the sum scores is between 0 and 15 points, their mean values are between 0 and 1.

For each method the sum and an average (i. e. sum divided by number of reported items) of all item scores was calculated. Reporting in included articles was evaluated by all three scoring methods.

Statistical analysis

The software package MedCalc version.19.0.7 was used. Descriptive statistics were calculated including the mean and standard deviation of each score, also the frequencies of score classes. Paired comparisons of each score were performed with the Mann-Whitney Test, agreement of scores in repeated evaluation were tested with Bland-Altman-plots.

Results

Included studies

Full versions of 3 articles out of 80 could not be retrieved [6,7,8]. 20 other articles were excluded from scoring, because they did not report skin temperature measurements in humans [9] or applied infrared thermal imaging in animal experiments [10,11]. Topical reviews on publications on thermology [12] and the use of thermal imaging for the detection of brown fat activity [13,14,15] were not considered for scoring. Also, educational material [16,17,18], editorials [19], comments on publications [2, 20,21,] or letters [22,23] were not analysed. Remaining exclusions were a paper on quality assurance in medical thermography [24] and a PhD thesis [25].

Scoring OS

3 recent articles [60, 73, 77] reached a maximal score, but complete reporting was not observed in articles retrieved from the review article by Vardasca [3]. The distribution of scoring classes found a higher proportion of complete reports in articles that quoted the TISEM checklist than in articles that did not cite (table 1). Item 14 ("method of drying the skin") was most frequently not applicable.

Comparing either the total OS1 or the averaged OS1 by using the Mann-Whitney-test found significant differences in favour of quoting articles (table 2, figure2).

Table 2
Ordinal scale 1(OS1) comparison between quoting articles and not quoting the TISEM checklist

	Total Ordinal Scale		Mean Ordinal Scale	
	Quoting	Non quoting	Quoting	Non quoting
Sample size	25	32	25	32
Lowest value	17	15	1.2	1.1
Highest value	45	38	3.0	2.7
Median	33	25.5	2.4	1.85
95% CI for the median	30.3 to 38.9	9.0 to 13.0	2.0 to 2.7	1.6 to 1.9
Interquartile range	28 to 41	8.0 to 14.5	1.6 to 1.95	1.6 to 1.9
Mann-Whitney t test (independent samples)				
Average rank of first group	38.9200		39.4600	
Average rank of second group	21.2500		20.8281	
Hodges-Lehmann median difference	8		0.6	
95% Confidenceinterval	5 to 12		0.3 to 0.8	
Mann-Whitney U	152.00		138.5	
Test statistic Z (corrected for ties)	-3.995		-4.223	
Two-tailed probability	p = 0.0001		p <0.0001	

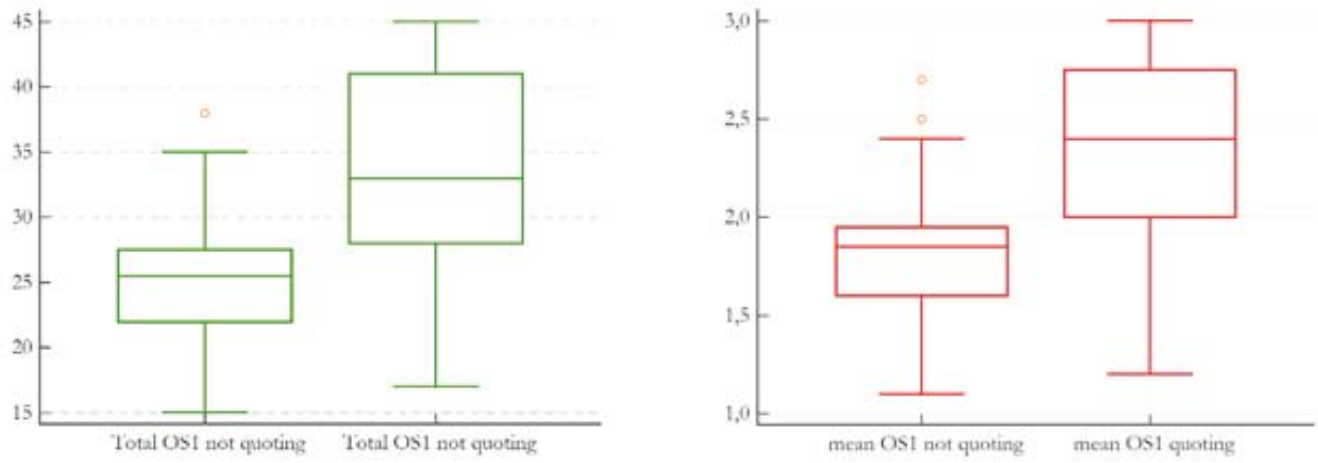

Figure 2
Box and whisker plots of the total and the mean OS1 scores in the TISEM quoting and not quoting group. The box represents the interquartile range, the line in the box the median and the whiskers mark extreme values.

Table 3
Comparison of total and mean OS2 scores between the scores in [4] and their repeated score.

	Total OS 2 in [4]	Total OS2 repeated	Mean OS 2 in [4]	Mean OS 2 repeated
Sample size	32	32	32	32
Lowest value	1	3	0.1	0
Highest value	28	24	1.9	1.7
Median	13.5	12	0.85	0.80
95% CI for the median	11.0 to 15.0	10.0 to 14.0	0.7 to 0.9	0.6 to 0.9
Interquartile range	10.0 to 16.5	8.0 to 15.0	0.7 to 1.1	0.6 to 0.9

Mann-Whitney t test (independent samples)

	Differences in the sum of scores	Differences in the mean scores
Average rank of first group	30.6250	33.2500
Average rank of second group	34.3750	30.7097
Hodges-Lehmann median difference	1	0
95% Confidence interval	-2 to 4	-0.2 to 0.1
Mann-Whitney U	452.0	456.0
Test statistic Z (corrected for ties)	-0.808	0.554
Two-tailed probability	p = 0.4193	p = 0.5793

Ordinal scale 2 (OS2)

The scoring of 32 articles retrieved from the article by Vardasca et al [4] was repeated and compared to the original scores using the Mann-Whitney-test. The result of this analysis is presented in table 3 and figure 3, showing slightly smaller scores in the repeated evaluation. The higher scores in [3] become less obvious in the comparison of the averaged OS2.

Identical total scores were observed in 4 cases only, in 11 cases was the repeated score higher than the original score and vice versa in the remaining 21 cases. Maximal differences were -9 and +17 points. A Bland Altman Plot found a wide range of limits of agreement and a mean bias to total agreement of -1.8 points (Figure 4).

Another comparison of the Ordinal Scale 2 (OS2) was in favour of articles that quoted the TISEM checklist indicating an improvement in complete reporting (Mann-Whitney: p=0.001)

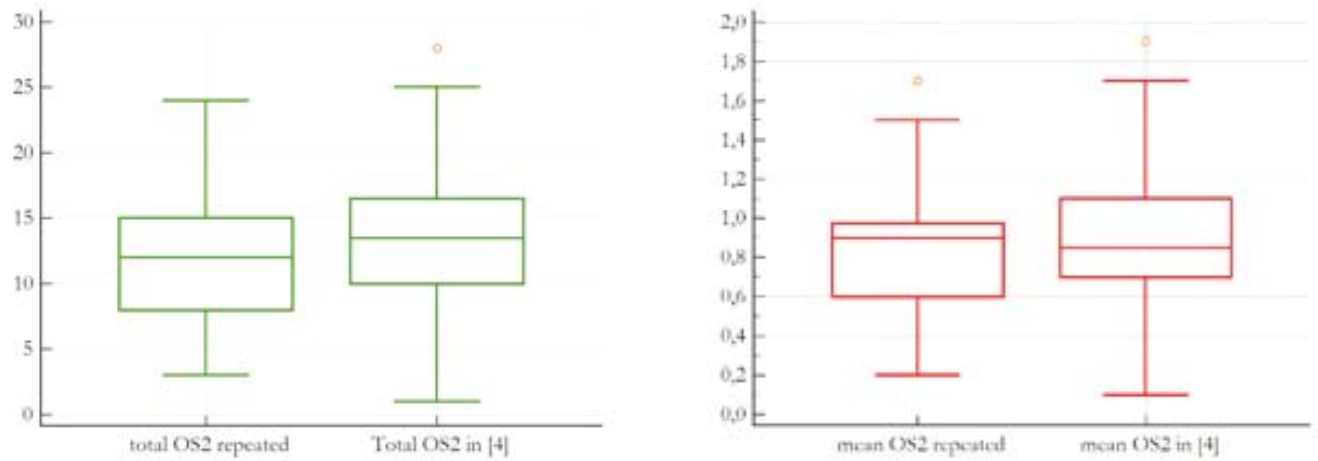

Figure3
Box and whisker plots of the total and mean OS2 scores in [4] in comparison to the repeated scoring

Figure 4
Agreement of the original total SQ scores with their repeated score values.

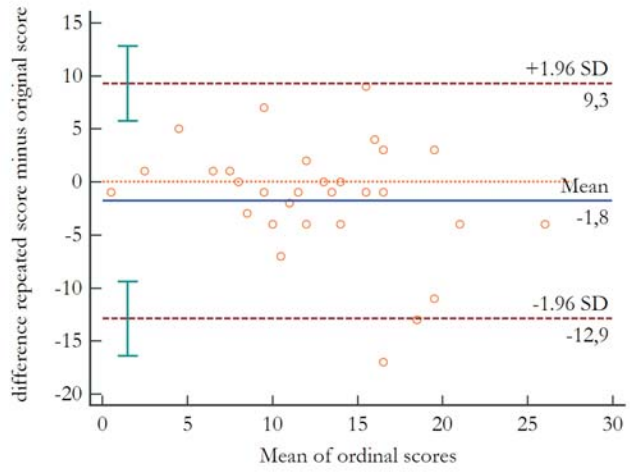

Quantitative Scale (QS)

Quantitative mean scoring resulted in a better description of incomplete reporting, because it generates an estimate percentage of completeness of reporting in articles which report the conditions of thermal imaging incompletely. Comparing QStotal and QSmean between TISEM quoting and TISEM not quoting articles confirmed that citing the TISEM significantly improves ($p<0.0001$) reporting in infrared imaging studies.

Comparison of all scores

Table 6 shows the mean values and standard deviation of all 3 scoring systems. In the group that quoted the TISEM checklist, the mean values of the ordinal scale 1 and the ordinal scale2 were by 0.5 points higher than in the non-citing group. The quantitative scale clearly indicates that TISEM quoting articles reached 70% completeness in reporting, whilst the rate of complete reporting was only 40% in the comparison.

Table 4
Quantitative scale comparison between articles quoting and not quoting the TISEM checklist

	Total QS not quoting	Total QS quoting	Mean QS not quoting	Mean QS quoting
Sample size	32	25	32	25
Lowest value	0.2	0.9	0.01	0.1
Highest value	12	15	0.9	1.0
Median	15.3	9.5	0.4	0.7
95% CI for the median	4.0 to 6.1	7.7 to 12.9	0.3 to 0.4	0.5 to 0.9
Interquartile range	3.7 to 6.7	7.0 to 13.2	0.3 to 0.5	0.5 to 0.9

Mann-Whitney t test (independent samples)

	Differences in the sum of scores	Differences in the mean scores
Average rank of first group	20.7500	20.5781
Average rank of second group	39.5600	39.7800
Hodges-Lehmann median difference	4.6	0.3
95% Confidence interval	2.8 to 6.6	0.2 to 0.5
Mann-Whitney U	136.00	130.50
Test statistic Z (corrected for ties)	-4.248	-4.366
Two-tailed probability	$p < 0.0001$	$p < 0.0001$

Figure5
Box and whisker plots of the total and the mean Q scores in the TISEM quoting and non quoting group

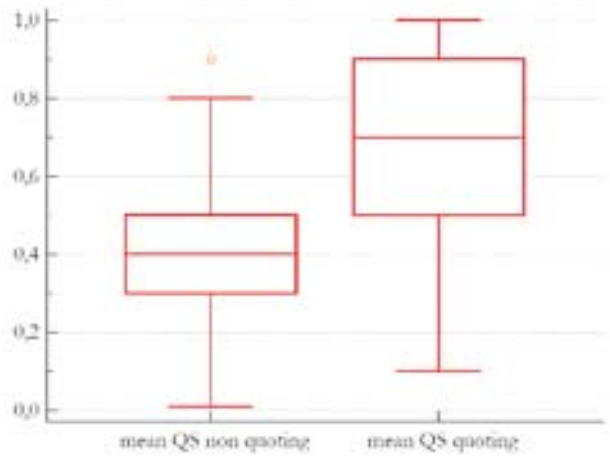

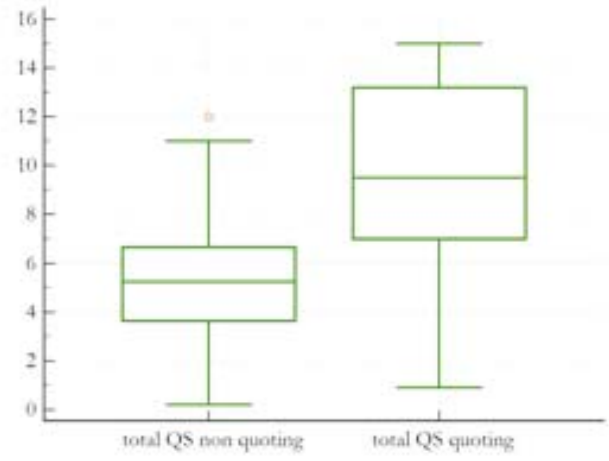

Table 6
Mean values and standard deviation of all scores (SD=standard deviation)

	TISEM quoting						Not TISEM quoting					
	$OS1_{total}$	$OS1_{mean}$	$OS2_{total}$	$OS2_{mean}$	Q_{total}	Q_{mean}	$OS1_{total}$	$OS1_{mean}$	$OS2_{total}$	$OS2_{mean}$	Q_{total}	Q_{mean}
mean	33.8	2.4	19.9	1.4	9.9	0.7	27.3	1.9	13.4	0.9	6.1	0.4
SD	7.3	0.5	7.3	0.5	3.7	0.2	7.5	0.4	5.3	0.4	2.8	0.2

Discussion

As previously shown [3,4], the TISEM checklist successfully identifies deficits in complete reporting of thermal imaging procedures. While the original scoring is done on a nominal scale, this scoring can be transformed to an ordinal scale or to a ratio scale. Particularly, the estimated percentage of complete reporting makes the interpretation of the score much easier than the class or the rank provided by the other two scoring methods.

The discrepancies between the scores reported by Vardasca et al [4] and the repeated scoring is a strong argument, that scoring should be performed by 3 persons, where the 3rd serves as referee in cases when consensus on scoring cannot be achieved. Main cause for inaccurate scoring is that required information may be overlooked despite it is available in the article, or that information was classified as present, although it was not. The attempt to quantify the content of each item by an estimate of completeness of reporting may be helpful in preventing non correct scoring. One may argue that assessing the scores from the current analysis with the scores obtained in [4] is an unfair comparison, because an unknown scoring process is related to the evaluation of a single observer. However, several examples of overlooked or as falsely present marked conditions raises the suspect, that scoring was performed in [4] by a single observer.

All 3 scoring methods support the impression, that the TISEM checklist is effective in improving the reporting, and indirectly the study design of thermal imaging studies. However, the TISEM should not be applied as a tool for the quality assessment of studies such as tools like QUADAS [81] or risk of bias tool of the Cochrane Collaboration [82] are used. The TISEM must be regarded as a tool to analyse the quality of reporting conditions that influence temperature reading obtained in thermal imaging studies. Thus, it is useful tool for assessing the uncertainty of temperature measurements based on infrared thermal imaging.

Since the TISEM requires reporting of processes and not to follow defined limits of environmental conditions, comparability of conditions should not be based on identical TISEM scores of two articles, because different conditions during infrared imaging may have been completely reported such as ambient temperature of 28° in one study and 18°C in the other study.

Nevertheless, high TISEM scores increase the credibility of reported temperature values, although the consistency of views, and body posture in serial thermal images cannot be derived from the TISEM score. Typically, views and posture are demonstrated by a template or an example image and deviations from this image in all recorded thermograms are rarely shown, even with TISEM recommending that a visual example of the standard body position of the subjects should be present (item 13). Studies on the reliability of positioning regions of interest are still rare, and studies on the reproducibility of body postures are even harder to find. Information on the reliability of these procedures is desirable, although not yet included in the TISEM.

There are two main limitations of this study. Scoring the articles by just one investigator is one of them, selection and comparison to historical score values obtained by unclear methodology is the other. Therefore, the reproducibility of the ordinal scale OS2 is only a rough estimate, and the repeatability of all 3 scoring methods remains unknown.

Definition of the search criteria for searching appropriate studies is quite a difficult task. Inclusion of clinical studies, that cite the TISEM article, is an obvious selection criterium if the study aim is the awareness of the checklist. But what features should be used in an investigation that is interested in the temporal improvement of reporting of thermal imaging studies? Ring and Ammer published in 2000 an article entitled "The Technique of Thermal Imaging in Medicine" [85], which mentioned already 14 of the 15 conditions included in the TISEM items [86]. Clinical papers, that quote the "technique article", might provide information on progress in reporting, if their TISEM score is compared to the scoring of TISEM citing articles.

Such a future study should involve three investigators, two of them should independently evaluate the identified "technique" and "TISEM" articles. The ordinal scale 1 and the quantitative scale should be applied. After each investigator has completed scoring, a consensual score should be formed, and permanent discrepancies will be resolved by the third investigator. The agreement of individual and consensual score values should be calculated, while different scores derived from "technique" or "TISEM" articles might indicate an improvement in reporting results of infrared imaging studies.

References

1.Moreira DG, Costello JT, Brito CJ, Adamczyk JG, Ammer K, Bach AJE, Costa CMA, Eglin C, Fernandes AA, Fernández-Cuevas I, Ferreira JJA, Formenti D, Fournet D, Havenith G, Howell K, Jung A, Kenny GP, Kolosovas-Machuca ES, Maley MJ, Merla A, Pascoe D, Priego- Quesada JI, Schwartz RG, Seixas ARD, Selfe J, Vainer BG, Sillero-Quintana M. Thermographic imaging in sports and exercise medicine: A Delphi study and consensus statement on the measurement of human skin temperature. Journal of Thermal Biology 2017; 69; 155-116

2.Moreira, DG, Costello, J.T, Brito, C.J, Sillero-Quintana, M. A checklist for measuring skin temperature with infrared thermography in sports and exercise medicine. Thermology International 2017, 27 (4) 136-138.

3.Ammer K. Sources of uncertainty in the evaluation of thermal images in medicine. In: Optical Methods for Inspection, Characterization, and Imaging of Biomaterials IV, edited by P. Ferraro, S. Grilli, M. Ritsch-Marte, CK. Hitzenberger, Proc. of SPIE 2019, Vol. 11060: 1106011-1106151

4.Vardasca R, Magalhaes C, Silva P, Abreu P, Mendes J, Restivo MT. Biomedical musculoskeletal applications of infrared thermal imaging on arm and forearm: A systematic review. Journal of Thermal Biology 2019, 82: 164-177

5.Ammer K. Does the TISEM-checklist address the deficits in reporting thermographic studies? Thermology international 2018, 28(2) 71

6.Al-Nakhli HH, Petrofsky, JS, Laymon MS, AraI D, Holland K, Berk LS. The use of thermal infrared imaging to assess the efficacy of a therapeutic exercise program in individuals with diabetes. Diabetes Technol Ther 2012, 14 (2), 159-167

7.Pérez-Guarner A, Priego-Quesada JI, Oficial-Casado F, Cibrián Ortiz De Anda RM, Carpes FP, Palmer RS. Association between physiological stress and skin temperature response after a half marathon. Physiological Measurement 2019, 40 (3), art. no. 034009,

8.Vainer BG. A Novel High-Resolution Method for the Respiration Rate and Breathing Waveforms Remote Monitoring. Annals of Biomedical Engineering 2018, 46 (7) 960-971.

9.Šegulja S, Ružic A, Dujmic D, Baždaric K, Roganovic J. Simple predictors of the reoccurrence of severe febrile neutropenia episode: A single center retrospective cohort study in pediatric patients with malignant diseases. Croatian Medical Journal 2019, 60 (1) 20-25

10.Pokorná J, Staffa E, Can V, Bernard V, Mornstein V, Farkašová M, Zetelolová A, Kala Z. Intestinal resection of a porcine model under thermographic monitoring. Physiological Measurement 2019, 40 (1), art. no. 014003,.

11.Bernard V, Staffa E, Can V, Farkašová M, Pokorná J, Mitáš L, Zetelová A, Mornstein V, Kala Z. Semi-Quantitative Comparison of Infrared Thermography with Indocyanine Green Imaging in Porcine Intestinal Resection. IRBM 2019.

12.Ammer K. Medical Thermology 2017 - A computer-assisted literature survey. Thermology International 2018, 28 (3) 139-178.

13.Law J, Chalmers J, Morris DE, Robinson L, Budge H, Symonds ME. The use of infrared thermography in the measurement and characterization of brown adipose tissue activation. Temperature 2018, 5(2), 147-161.

14.Law J, Morris DE, Budge H, Symonds ME. Infrared thermography. Handbook of Experimental Pharmacology 2019, 251 259-282.

15.Levy SB. Field and laboratory methods for quantifying brown adipose tissue thermogenesis. American Journal of Human Biology 2019, art. no. e23261.

16.Carpes FP, Mello-Carpes PB, Priego-Quesada JI, Pérez- Soriano P, Palmer RS, de Anda RMCO. Insights on the use of thermography in human physiology practical classes. Advances in Physiology Education 2018, 42 (3) 521-525.

17.Ammer K. Producing a thermographic report. Thermology International 2018, 28 (1), p. 19.

18.Seixas A. Educational resources. Thermology International 2018, 28 (1) 22-24.

19.Ammer K. One step closer to evidence based infrared thermal imaging. Thermology International 2017, 27 (4) 125-126.

20.Seixas, A. Stockings, running and thermal imaging. Thermology International 2019, 29 (1) 5-6.

21.Seixas A, Ammer K. Reliability of the analysis of infrared thermography images. Thermology International 2018, 28 (4) 192-193.

22.Seixas A, Ammer K. Utility of infrared thermography when monitoring autonomic activity. European Journal of Applied Physiology 2019, 119(6) 1455-1456.

23.Rakobowchuk M. Reply to the Letter to the Editor: Utility of lacrimal caruncle infrared thermography when monitoring alterations in autonomic activity in healthy humans. European Journal of Applied Physiology 2019, 119(6) 1459-1460.

24.Marjanovic EJ, Britton J, Howell KJ, Murray AK. Quality assurance for a multi-centre thermography study. Thermology International 2018, 28 (1) 7-13.

25.Priego-Quesada JI. THERMOBIKE: Applicability of infrared thermography in the assessment of the efficiency, performance, and posture of the cyclist. PhD Thesis, University of Valencia 2017.

26.Abate M, Di Carlo L, Di Donato L, Romani GL, Merla A, Comparison of cutaneous thermic response to a standardised warm up in trained and untrained individuals J Sports Med Phys Fitness. 2013;53(2):209-15.

27.Aquilar TAC, Manrique BV, Torrejon JA, Development of a mechatronic device for arm rehabilitation Sistemas Embebidos Aplicaciones y Tendencias 2016, 23-28.

28.Al-Nakhli HH, Petrofsky, JS, Laymon MS, Berk LS. The use of thermal infrared imaging to detect delayed onset muscle soreness. JoVE 2012 (59), 3551.

29.Bartuzi P, Roman-Liu, D, Wisniewski T. The influence of fatigue on muscle temperature. Int J Occup Saf Ergon 2012, 18 (2), 233-243.

30.Boguszewski D, Adamczyk JG, Andersz N, Mrozek N, Piejko K, Janicka M, Bialoszewski D. Impact of classical massage on temperature strength and flexibility of upper limbs muscles in healthy men. Trends in Sport Sciences 2015; 22 (2) 71-75.

31.Chang K, Yoon S, Sheth N, Seidel M, Antalek M, Ahad J, Darlington T, Ikeda A, Kato GJ, Ackerman H, Gorbach AM, Rapid vs delayed infrared responses after ischemia reveal recruitment of different vascular beds. Quantitative Infrared Thermography Journal 2015; 12 (2) 173-183.

32.Chudecka M, Lubkowska A. Temperature changes of selected body's surfaces of handball players in the course of training estimated by thermovision and the study of the impact of physiological and morphological factors on the skin temperature. J Therm Biol 2010, 35 (8), 379-385.

33.Chudecka M, Lubkowska A. The use of thermal imaging to evaluate body temperature changes of athletes during training and a study on the impact of physiological and morphological factors on skin temperature. Hum Mov 2012. 13 (1), 33-39.

34.Curkovic S, Antabak A, Halužan D, Luetic T, Prlic I, Šiško J. Medical thermography (digital infrared thermal imaging-DITI) in paediatric forearm fractures-A pilot study. Injury 2015. 46, S36-S39.

35.Gabrhel J, Popracova Z, Tauchmannova H, Ammer K. The role of infrared thermal imaging and sonography in the assessment of patients with a painful elbow. Thermology International 2017, 27 (2), 58-66.

36.Galvin EM, Niehof, S, Medina HJ, Zijlstra FJ, van Bommel J, Klein J, Verbrugge SJ. Thermographic temperature measurement compared with pinprick and cold sensation in predicting the effectiveness of regional blocks Anesth Analg 2006, 102 (2), 598-604.

37.Haluzan D, Davila S, Antabak A, Dobric I, Stipic J. Augustin G, Prlic I. Thermal changes during healing of distal radius fractures - preliminary findings. Injury 2015 46, S103-S106.

38.Herry, CL, Frize M, Goubran RA, Comeau, G. Evolution of the surface temperature of pianists' arm muscles using infrared thermography In: Engineering in Medicine and Biology Society, IEEE-EMBS 2005 27th Annual International Conference of the IEEE, pp 1687-1690.

39.Jaworski L, Siondalski P, Jarmoszewicz K, Rogowski J. Arm temperature distribution in thermographic pictures after radial artery harvesting for coronary bypass operation. Interact Cardiovasc Thorac Surg 2007, 6 (5), 598-602.

40.Lampe R, Kawelke S, Mitternacht J, Turova V, Blumenstein T, Alves A. Thermograpic study of upper extremities in patients with cerebral palsy. Opto-Electron Rev 2015, 23 (1), 62-67

41.Lange KHW, Jansen T, Asghar S, Kristensen PL, Skjonnemand M, Norgaard P. Skin temperature measured by infrared thermography after specific ultrasound-guided blocking of the musculocu taneous radial ulnar and median nerves in the upper extremity. Br J Anaesth 2011, 106 (6), 887-895

42.Magalhaes MF, Dibai-Filho AV, de Oliveira Guirro EC, Girasol CE, de Oliveira AK, Dias FRC, de Jesus Guirro RR. Evolution of skin temperature after the application of compressive forces on tendon muscle and myofascial trigger point PLoS One 2015, 10 (6), e0129034

3.Merla A, Mattei PA, Di Donato L, Romani GL. Thermal imaging of cutaneous temperature modifications in runners during graded exercise. Ann Biomed Eng 2010, 38(1) 158-163.

44.Mohamed S, Frize M, Comeau G. Assessment of piano-related injuries using infrared imaging In: Engineering in Medicine and Biology Society, EMBC, 2011 Annual International Conference of the IEEE, pp 4901-4904.

45.Neves EB, Vilaca-Alves J, Moreira TR, Reis VM. The thermal response of biceps brachii to strength training Gazz Med Ital 2016, 175 (10), 391-399.

46.Neves EB, Moreira TR, Lemos RJ, Vilaca-Alves J, Rosa C, Reis VM. The influence of subcutaneous fat in the skin temperature variation rate during exercise. Res Biomedical Eng 2015, 31 (4), 307-312.

47.Neves EB, Bandeira F, Ulbricht L, Vilaca-Alves J, Reis VM. Influence of muscle cross-sectional area in skin temperature. In: Proceedings of the International Conference on Bioimaging (BIOIMAGING-2015) 2015, pp 64-68.

48.Novotny, J, Rybarova S, Zacha D, Novotny, J, Bernacikova M, Ramadan WA, The influence of breaststroke swimming on the muscle activity of young men in thermographic imaging Acta Bioeng Biomech 2015, 17 (2), 121-129.

49.Park JY, Hyun JK, Seo JB. The effectiveness of digital infrared thermographic imaging in patients with shoulder impingement syndrome J Shoulder Elb Surg 2007, 16 (5), 548-554.

50.Ratovoson D, Jourdan F, Huon V. Influence of gravity on the skin thermal behavior: experimental study using dynamic infrared thermography Skin Res Technol 2013, 19 (1), 397-408.

51.Reste J, Zvagule T, Kurjane N, Martinsone Z, Martinsone I, Seile A, Vanadzins I. Wrist hypothermia related to continuous work with a computer mouse: a digital infrared imaging pilot study Int J Environ Res Public Health 2015, 12 (8) 9265-9281.

52.Rossignoli I, Fernandez-Cuevas I, Benito PJ, Herrero AJ..Relationship between shoulder pain and skin temperature measured by infrared thermography in a wheelchair propulsion test. Infrared Phys. Technol 2016, 76, 251-258.

53.Sefton JM, Yarar C, Berry JW, Pascoe DD. Therapeutic massage of the neck and shoulders produces changes in peripheral blood flow when assessed with dynamic infrared thermography. J. Altern. Complement. Med. 2010,16 (7) 723-732.

54.Silva CT, Naveed N, Bokhari S, Baker KE, Staib LH, Ibrahim SM, Muchantef K, Goodman TR. Early assessment of the efficacy of digital infrared thermal imaging in pediatric extremity trauma. Emerg. Radiol. 2012,19 (3), 203-209.

55.Thomas D, Siahamis G, Marion M, Boyle C. Computerised infrared thermography and isotopic bone scanning in tennis elbow. Ann. Rheum. Dis. 1992, 51 (1), 103-107.

56.Trentin MG, Oliveira GA, Setti D. Thermography: an a assessment tool in the ergonomic analysis of a workstation in the foundry industry. In: Proceedings of the XVIII International Conference on Industrial, Guimaraes, Portugal, 2012, pp. 9-11.

57.Vardasca R, Restivo MT, Mendes J. Skin temperature bilateral differences at upper limbs and joints in healthy subjects. In: European Congress on Computational Methods in Applied Sciences and Engineering 2018. Springer, Cham., vol. 27, pp. 1005-1010

58.Cabizosu A, Carboni N, Figus A, Vegara-Meseguer JM, Casu G, Hernández Jiménez P, Martinez-Almagro Andreo A. Is infrared thermography (IRT) a possible tool for the evaluation and follow up of Emery-Dreifuss muscular dystrophy? A preliminary study. Medical Hypotheses2019, 127 91-96.

59.Costa CMA, Moreira DG, Sillero-Quintana M, Brito CJ, de Azambuja Pussieldi G, de Andrade Fernandes A, Cano SP, Bouzas Marins JC. Daily rhythm of skin temperature of women evaluated by infrared thermal imaging. Journal of Thermal Biology 2018, 72 1-9.

60.Danek JW, Flosadóttir S. Effects of physical exercise in winter training conditions on the thermographic temperature distribution of the horse rider's skin. Acta of Bioengineering and Biomechanics 2018, 20 (3) 133-137.

61.de Andrade Fernandes A, Pimenta EM, Moreira DG, Sillero-Quintana M, Marins JCB, Morandi RF, Kanope T, Garcia ES. Skin temperature changes of under-20 soccer players after two consecutive matches. Sport Sciences for Health 2017, 13 (3) 635-643.

62.Diaz-Piedra C, Gomez-Milan E, Di Stasi LL. Nasal skin temperature reveals changes in arousal levels due to time on task: An experimental thermal infrared imaging study Applied Ergonomics 2019, 81, art. no. 102870, .

63.Carbonell L, Priego Quesada JI, Retorta P, Benimeli M, Cibrián Ortiz De Anda RM, Salvador Palmer R, González Peña RJ, Galindo C, Pino Almero L, Blasco MC, Mínguez MF, Macián-Romero C. Thermographic quantitative variables for diabetic foot assessment: preliminary results. Computer Methods in Biomechanics and Biomedical Engineering: Imaging and Visualization, 2018. Article in Press.

64.Eglin CM, Costello JT, Bailey SJ, Gilchrist M, Massey H, Shepherd AI. Effects of dietary nitrate supplementation on the response to extremity cooling and endothelial function in individuals with cold sensitivity. A double blind, placebo controlled, crossover, randomised control trial. Nitric Oxide - Biology and Chemistry 2017, 70, 76-85.

65.da Silva W, Machado ÁS, Souza MA, Kunzler MR, Priego-Quesada JI, Carpes FP. Can exercise-induced muscle damage be related to changes in skin temperature? Physiological Measurement 2018, 39(10) 104007.

66.Gil- Calvo M, Priego-Quesada JI , Jimenez-Perez I, Lucas-Cuevas A, Soriano PP. Effects of prefabricated and custom-made foot orthoses on skin temperature of the foot soles after running. Physiological Measurement 2019, 40: 054004.

67.Gruszka K, Szczuka E, Calkosinski, I, Sobiech KA, Chwalczynska, A. Thermovision analysis of surface body temperature changes after thermal stimulation treatments in healthy men. Acta of Bioengineering and Biomechanics 2018, 20 (2) 79-87.

68.Kasprzyk T, Cholewka A, Kucewicz M, Sieron, K, Sillero-Quintana M, Morawiec T, Stanek A. A quantitative thermal analysis of cyclists' thermo-active base layers. Journal of Thermal Analysis and Calorimetry 2019, 136 (4) 1689-1699.

69.Da Silva W, Machado AS, Souza MA, Kunzler MR, Priego-Quesada JI, Carpes FP. Can exercise-induced muscle damage be related to changes in skin temperature? Physiological Measurement 2018; 39 (10), art. no. 104007.

70.Martinez-Jimenez MA, Ramirez-GarciaLuna JL, Kolosovas-Machuca ES, Drager J, Gonzalez FJ. Development and validation of an algorithm to predict the treatment modality of burn wounds using thermographic scans: Prospective cohort study. PLoS ONE 2018; 13(11): e0206477.

71.Moliné A, Fernández-Gómez J, Moya-Pérez E, Puertollano M, Gálvez-García G, Iborra O, Gómez-Milán E. Skin temperature reveals empathy in moral dilemmas: An experimental thermal infrared imaging study. Thermology International 2018, 28 (4) 197-206.

72.Moreira DG, Molinari AB, Fernandes AA, Sillero-Quintana M, Brito CJ, Doimo LA, Marins JCB. Skin temperature of physically active elderly and young women measured using infrared thermography. Journal of Physical Education and Sport, 2017, 17 (4), art. no. 286 2531-2537.

73.Moreira-Marconi E, Moura-Fernandes MC, Lopes-Souza P, Teixeira-Silva Y, Reis-Silva A, Marchon RM, De Oliveira Guedes-Aguiar E, Paineiras-Domingos LL, Da Cunha De Sá-Caputo D, Morel DS, Dionello CF, De-Carvalho SO, Dos Santos Pereira MJ, Francisca-Santos A, Silva-Costa G, Olímpio-Souza M, Lemos-Santos TR, Asad NR, Xavier VL, Taiar R, Sonza A, Seixas A, Cochrane DJ, Bernardo-Filho M. Evaluation of the temperature of posterior lower limbs skin during the whole-body vibration measured by infrared thermography: Cross-sectional study analysis using linear mixed effect model. PLoS ONE 2019, 14 (3), art. no. e0212512.

74.Moreira-Marconi E, Soares Morel D, Oliveira de-Carvalho S, Paineiras-Domingos LL, Cunha Sá-Caputo D, dos Santos Pereira MJ, Moura-Fernandes MC; Machado e Silva JR, Seixas A, Taiar R, Bernardo-Filho M. The role of infrared image in the assessment of early effects of a mosquito bite: a brief report. Series on Biomechanics 2018, 32(3) 47-51.

75.Norheim AJ, Borud,E, Wilsgaard T, De Weerd L, Mercer JB. Variability in peripheral rewarming after cold stress among 255 healthy Norwegian army conscripts assessed by dynamic infrared thermography. International Journal of Circumpolar Health 2018, 77 (1) art. no. 1536250.

76.Oliveira SAF, Marins JCB, Da Silva AG, Brito CJ, Moreira DG, Sillero-Quintana M. Measuring of skin temperature via infrared thermography after an upper body progressive aerobic exercise. Journal of Physical Education and Sport 2018, 18 (1) 184-192.

77.Raccuglia, M, Heyde, C, Lloyd, A, Hodder, S, Havenith, G. The use of infrared thermal imaging to measure spatial and temporal sweat retention in clothing. International Journal of Biometeorology 2019, 63: 885-894

78.Rodríguez-Sanz D, Becerro-de-Bengoa-Vallejo R, Losa-Iglesias M, Martínez-Jiménez E, Muñoz-García D, Pérez- Boal E, Calvo-Lobo C, López-López D. Effects of compressive stockings and standard stockings in skin temperature and pressure pain threshold in runners with functional ankle equinus condition. Journal of Clinical Medicine, 2018, 7(11) 454.

79.Seixas A, Mendes J, Vardasca R, Bernardo-Filho M, Rodriguesa S. Immediate effects of whole-body vibration exercise on thermal symmetry of the lower legs and ankles. Revista HUPE, Rio de Janeiro, 2018;17(1):26-33.

80.Shida N, Furukawa Y, Nitta O. Skin Temperature Responses in a Hot Environment among Wheelchair Rugby and Basketball Players with Spinal Cord Injury. Int J Phys Med Rehabil 2018; 6: 478.

81.Vainer BG. Up-to-Date Thermal Imaging Systems in the Multichannel Automated Measurements. In: 2018 14th International Scientific-Technical Conference on Actual Problems of Electronic Instrument Engineering, APEIE 2018 - Proceedings, art. no. 8546318 334-338.

82.Weigert M, Nitzsche N, Kunert F, Lösch C, Schulz H. The influence of body composition on exercise-associated skin temperature changes after resistance training. Journal of Thermal Biology2018, 75 112-119.

83.Whiting PF, Rutjes AW, Westwood ME, Mallett S, Deeks JJ, Reitsma JB. et al. QUADAS-2: a revised tool for the quality assessment of diagnostic accuracy studies. Annals of Internal Medicine 2011, 155(8), 529-536.

84.Higgins JP, Altman DG, Gøtzsche PC, Jüni P, Moher D, Oxman AD et al. The Cochrane Collaboration's tool for assessing risk of bias in randomised trials. BMJ 2011; 343: d5928.

85.Ring EFJ, Ammer K The technique of infrared imaging in medicine. Thermology international 2000; 10(1) 7-14

86.Ammer K. The Most Cited Article from Thermology International In The Period 2000 To 2018. Thermology international 2019; 29(2) 62

Address for Correspondence

Prof Dr med Kurt Ammer PhD

European Association of Thermology

1170 Vienna, Austria

(Received 09.08.2019, revision accepted 10.09.2019)

The reliability of an Achilles tendon infrared image analysis method

Ben Oliver. A Munro, S. Gerald, L. Herrington

Salford University School of Health and Society, Salford, United Kingdom

SUMMARY

INTRODUCTION: Prior to utilising smartphone-based thermal imaging for clinical assessment of the Achilles tendon, the intra-rater and inter-rater reliability of the method of analysis must be established, with associated standard error of measurement (SEM) and minimal detectable change (MDC) values.

METHOD: A convenience sample of 7 participants (4male, 3female, age 18.57± 1.57 years, height 173.7 ± 6.3cm, weight 73.8 ± 8.1kg) were recruited for the study, for a total of 28 skin temperature (TSk) measurements per camera. Measurements were taken using two infrared cameras, one handheld (FLIR E8) and one smartphone-compatible (FLIR ONE), from 0.5m and 1m distances. Regions of interest (ROI) were retrospectively selected using a freeform software ROI tool.

RESULTS: The method used to analyse TSk of the midportion of the Achilles tendon demonstrated excellent intra-rater reliability at both 0.5m and 1m distances using the FLIR ONE (ICC = 0.99, ICC = 0.99) and FLIR E8 (ICC = 0.98, ICC = 0.95). There was excellent inter-rater reliability of the method at 0.5m and good inter-rater reliability at 1m with data captured from the FLIR ONE (ICC = 0.97, ICC = 0.79), and excellent ICC's at both distances for the FLIR E8 (ICC = 0.97, ICC = 0.99).

CONCLUSIONS: The method of TSk analysis using the FLIR ONE is acceptable at 0.5m and 1m distances, however data capture is recommended for the closer distance.

KEYWORDS: Thermography, Achilles tendon, reliabilty

DIE ZUVERLÄSSIGKEIT EINER METHODE ZUR ANALYSE VON INFRAROT-WÄRMEBILDERN DER ACHILLESSEHNE

EINLEITUNG: Vor der Nutzung von mit dem Smartphone aufgenommenen Wärmebildern zur klinischen Beurteilung der Achillessehne muss für gleiche und unterschiedliche Untersucher die Zuverlässigkeit der Analysemethode mit dem damit verbundenen Standardfehler der Messung (SEM) und minimalen MDC-Werten (erkennbarer Unterschied) bekannt sein..

METHODE: Für die Studie wurde eine willkürliche Stichprobe von 7 Teilnehmern (4 männlich, 3 weiblich, Alter: 18,5 7± 1,57 Jahre, Körpergröße: 173,7 ± 6,3 cm, Gewicht 73,8 ± 8,1 kg) rekrutiert, um pro Kamera insgesamt 28 Temperaturmessungen (TSk) durchzuführen. Die Messungen wurden mit zwei Infrarotkameras, einer tragbaren FLIR E8 und einer Smartphone-kompatiblen FLIR ONE aus 0,5m und 1m Entfernung durchgeführt. Die Auswerteareale (ROI) wurden rückblickend mit einer geeigneten Software ausgewählt.

ERGEBNISSE: Die Methode zur Analyse der TSk über dem mittleren Anteil der Achillessehne zeigte bei 0,5m und 1m Entfernungen Zuverlässigkeit bei gleichen Untersuchern eine ausgezeichnete für die FLIR ONE (ICC = 0.99, ICC = 0.99) und die FLIR E8 (ICC = 0.98, ICC = 0.95). Es zeigte sich für unterschiedliche Untersucher eine ausgezeichnete Zuverlässigkeit der Methode bei 0,5m und eine gute Zuverlässigkeit bei 1m für Daten, die mit der FLIR ONE erhoben wurden (ICC = 0,97, ICC = 0,79) und ausgezeichnete ICC-Werte bei beiden Entfernungen für die FLIR E8 (ICC = 0,97, ICC = 0,99).

SCHLUSSFOLGERUNG: Die Methode der TSk-Analyse mit der FLIR ONE ist bei 0,5m und 1m Entfernung akzeptabel, jedoch wird die Datenerfassung der nähere Abstand empfohlen.

SCHLÜSSELWÖRTEr: Thermographie, Achillessehne, Zuverlässigkeit

Thermology international 2019, 29(4) 136-145

Introduction

Achilles tendinopathy is a condition which has been shown to affect up to 57% of running populations [1]. The condition is prevalent throughout other sports, having accounted for 96% of all Achilles tendon disorders in elite male football [2] and led to a higher total absence from training and match play than any other ankle injury in rugby union [3]. The incidence of Achilles tendinopathy in the general population has been reported at 2.35 per 1000 registered across a number of General Practices [4].

The pathophysiology of the condition is complex and not fully understood. Specifically, midportion Achilles tendinopathy is characterised by pain, swelling 2-6cm proximal to the insertion on the calcaneus, and reduced performance, all of which are cardinal signs of inflammation [5-7]. Research has recently shifted from the assumption that Achilles tendinopathy was purely a degenerative condition, to acknowledging that inflammatory cells are present in symptomatic tendons, however it is important to note that

physiologically these cells differ from those associated with a typical acute response [5].

Biomechanical alterations have been proposed to contribute to the onset of Achilles tendinopathy, two of these being alterations to strain and stiffness of the tendon [8,9]. Alterations to these biomechanical properties will result in a more compliant tendon, which is less efficient in returning stored elastic energy, and greater energy being dissipated via heat, termed mechanical hysteresis, a hypothesis which was proven in symptomatic tendons by Wang et al [10].

The presence of both inflammatory cells and hysteresis within the Achilles tendon may be indicated by some degree of thermal change, a concept that has been established previously in equine thermography [11]. This idea provided the foundation to investigate whether thermal change exists at the surface of the skin over the Achilles tendon, using a device that can track skin temperature (TSk).

Infrared thermography provides a non-invasive method of detecting changes in temperature from local regions of skin [12,13] and has been utilised since the mid-twentieth century for medical assessment purposes. It has replaced traditional contact measurement devices for the measurement of TSk, however, there has been a debate about the usability of the technology, with some authors demonstrating poor concurrent validity [14-16].

In these studies [14-16], the contact devices were secured to the skin of the participants using tape, which could influence local TSk values through the creation of a microclimate. Quesada et al. [17] demonstrated that when using tape to secure the contact device, a TSk difference (δT) of 0.5°C existed between a thermal camera and an iButton, however, when the iButton was left uncovered, no δT existed. Strong correlation was found between the thermal camera and iButton prior to, during and after an exercise intervention [17], indicating excellent concurrent validity when infrared thermal imaging cameras are used to monitor TSk in response to exercise.

As technology has improved, smartphone-based thermal imaging cameras have become increasingly popular, but the question exists again regarding their validity. One such device, the FLIR ONE, is deemed to have a lower specification than most handheld devices (table 1), with lower accuracy, infrared resolution (IR resolution), spatial resolution (instantaneous field of view - IFOV) and thermal sensitivity. Definitions of these terms can be found in table 2. Despite this, excellent criterion and convergent validity have been demonstrated for the FLIR ONE when compared against other TSk measurement devices [18,19].

The improvement in technology has seen the introduction of Multi-Spectral Dynamic imaging, which is a patented technology created by FLIR systems. It combines two pictures taken by the same camera, a digital image with a regular thermal image and enhances the latter with the addition of outline detail. This allows visible spectrum features to be intertwined with those of the long-infrared range of the electromagnetic spectrum [20], creating an image with a greater number of pixels than just the thermal image alone. This is the case with the FLIR ONE infrared thermal imaging camera, which has a thermal resolution of 120 x 160 pixels pixels but a pixel count of 480 x 640 when combined with MSX technology. It is important to clarify that MSX technology does not enhance the thermal resolution of the IR camera, but it interpolates the thermal and digital images to create a temperature point every 4x4 pixels.

Despite its lower thermal specification, the FLIR ONE has been shown to have excellent reliability [18,21,22], however only one study has reported the standard error of measurement (SEM) which was 0.22°C [22], but no study has reported the minimal detectable change (MDC). It is im-

Table 1
The specification of the FLIR ONE and FLIR E8 infrared thermal imaging cameras

Specification	FLIR E8	FLIR ONE
IR Resolution	320x240	160x120
MSX Resolution	320x240	640x480
Accuracy	± 2%	±5%
FOV (Horizontal/Vertical)	45°x°34	46°x35°
Spatial Resolution (IFOV)	2.6mrad	11.6mrad
Thermal Sensitivity	<60mK	150mK
Spectral Range	7.5-13µm	8-14µm
Minimum Focus Distance	0.5m	0.3m

Table 2
Definitions of infrared thermal imaging terms

Accuracy	The manufacturer stated percentage difference in a measured temperature and the known temperature of a reference source
IR resolution	The number of pixels contained within an image. One pixel is one temperature datum point.
Field of view (FOV)	The largest area that an infrared thermal camera can detect
Minimum focus distance	The smallest distance from an object at which the lens of the camera is able to focus
MSX technology	The combination of an infrared thermal image and a digital image to create a single infrared thermal image with skeletonised digital detail
Instantaneous field of view (IFOV)	Often termed spatial resolution.An angular projection of one single pixel in the infrared image
Spectral range	The wavelength range that the infrared thermal imaging camera can detect
Thermal sensitivity	The smallest difference in temperature that an infrared thermal imaging camera can detect over temporal noise

portant to report the SEM of the thermal imaging cameras so that we know the standard deviation (SD) of the errors of measurement around measured TSk values, and the MDC allows us to understand values of ΔT that are required for statistically significant TSk change that is not associated with error. Kanazawa et al. [18] used the Cohen's kappa coefficient statistic to assess criterion validity, intra-rater and inter-rater reliability. Cohen's kappa coefficient is used with categorical variables, so the researchers have categorised temperature measurements as being higher or lower at the wound bed than at the skin of the peri wound. It is important not to rely solely on the results of this study if assessing absolute TSk changes as the results are based on categorical data analysis. It would be expected that two devices measuring skin temperature would detect whether a temperature is higher or lower than another point. It may have been more appropriate to include intra-rater and inter-rater reliability analysis using intraclass correlation coefficients (ICC's) on a continuous scale using obtained temperature values alongside categorical classifications in order to reflect the clinical application of the FLIR ONE device and to use Bland-Altman analysis to determine whether devices agree with each other [23,24].

Moreira et al. [25] conducted a Delphi study and produced the Thermographic imaging in sports and exercise medicine (TISEM) checklist which has helped to standardise methodology and improve reporting standards of thermal imaging studies, which will ultimately increase the reproducibility of thermal imaging studies.

Therefore, the aims of the current study were to determine the intra-rater and inter-rater reliability of the method of TSk analysis at 0.5m and 1m distances, with associated SEM's and MDC's for both devices. The agreement between the devices will also be assessed.

Method

Testing was conducted at the University Human Performance Laboratory. Ethical approval was granted by the University Research, Enterprise and Engagement Ethical Approval Panel (HSR1718-032).

Participants

A convenience sample of 7 participants were recruited for this study (4male, 3female; age 18.6± 1.6 years, height 173.7± 6.3cm, weight 73.8± 8.1kg) based upon the paper by Bujang and Baharum [26]. All of the participants were University students who volunteered to participate following a poster recruitment campaign. Participants were eligible to partake if they met a strict inclusion and exclusion criteria. Participants were required to adhere to strict pre-participation criterion. Prior to any of the testing sessions, participants were instructed to avoid consumption of alcoholic beverages, caffeine products and to avoid smoking on the day of testing. Participants were asked not to eat a large meal in the four hours prior to testing. Participants were asked not to apply any lotions or cosmetics to their skin on the day of testing and they were asked not to shower within 4 hours of testing. Participants completed a Physical Activity Readiness Questionnaire (PAR-Q) which confirmed that they were not taking any medication, along with details regarding the level, duration and times of their last exercise-based activities.

The 7 participants were tested across two days. Testing was conducted with overhead lighting turned off to minimise reflection, and in a location whereby external conditions would not affect TSk. Room temperature and humidity were recorded using a digital weather station. The mean ambient room temperature was 22.17°C (± 0.17°C) and the humidity was 40.47% (± 1.51%).

Experimental setup

A black polycotton sheet was hung to provide a smooth dark background and a piece of foil was placed on this sheet so that reflected temperature could be measured. A line of tape was placed parallel to this, on the floor, with the furthest edge of the tape 40cm in front of the sheet. Participants stood with their heels at the edge of the tape in the anatomical position, with their feet 24cm apart.

A grid of tape was then constructed, with four camera placement points at 0° perpendicular to the regions of interest (ROI) on the Achilles tendons, at 0.5m and 1m distances. This can be seen in Figure 1.

Testing was conducted with both the FLIR ONE (2nd Generation) and the FLIR E8 infrared thermal imaging cameras. Their specifications can be seen in table 1.

The FLIR E8 was switched on 60 minutes prior to data collection to stabilise at room temperature, however, this was not possible with the FLIR ONE due to its short battery life. Instead, the camera was left off during this period and switched on at the beginning of the 15-minute acclimatisation period. The emissivity of both cameras was set to 0.98.

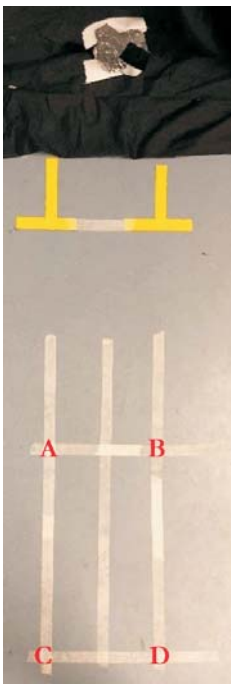

Figure 1
Tape grid with camera locations

A= Left leg TSk measure at 0.5m
B = Right leg TSk measure at 0.5m
C = Left leg TSk measure at 1m
D = Right leg TSk measure at 1m

The cameras were placed perpendicular (0° angle) to the tape markers (Figure 1 positions A, B, C & D) where the participants stood, at a distance of 0.5m or 1m, in front of the left or right leg. The placement order was block randomised for each participant, with both legs being measured at both distances. The FLIR E8 was mounted to a clamp at a height of 0.21m, the lowest due to the height of the camera. It was connected via USB cable to a laptop, which was used to take the images, using FLIR Research IR MAX (v4.40.9.30, FLIR Systems, Oregon, US). The FLIR ONE was mounted on a tripod also at a 0.21m height to replicate the placement of the FLIR E8.

Upon attendance at the laboratory, participants had their anthropometrics measured. They then underwent a 15-minute acclimatisation period in line with the recommendations set by Moreira et al. (2017) [25]. During this time, 4 thermally inert markers were stuck to the skin of the participants at the following anatomical landmarks: insertion of the Achilles tendon on the posterior tuberosity of the calcaneus, the musculotendinous junction of the heads of the Gastrocnemius and both the medial and lateral malleoli (figures 2 and 3). These landmarks were identified through palpation, with the participant standing in the anatomical position. All of these anatomical landmarks were located via palpation in the standing anatomical position.

After the 15-minute acclimatisation period, images were taken of the left and right legs of the participants from locations A & B (0.5m) and C & D (1m) as seen in figures 1 and 2, using both the FLIR ONE and the FLIR E8.

Data analysis

There were a total of 28 TSk measurements captured per camera, 14 at a 0.5m distance (7 at position A and 7 at position B) and 14 at a distance of 1m (7 at position C and 7 at position D). Thermal images from the FLIR E8 were stored on the laptop that was connected to the thermal camera, and on the smartphone for those captured by the FLIR ONE. The FLIR ONE images were then retrospectively transferred to the laptop for analysis.

Retrospective analysis of the thermal images was conducted using FLIR Research IR MAX (v4.40.9.30, FLIR Systems, Oregon, US). A freeform ROI was drawn between the distal and proximal anatomical markers, with the examiners judging the line to trace through the centre of the Achilles tendon. The line was then exported into Microsoft Excel (v16.0, Microsoft corporation, WA, US) in the format of a comma-separated values file (CSV). A 2cm distance was then determined in the CSV file based on the number of pixels equating to the known diameter of the anatomical marker in FLIR Research IR Max. The start points for calculating the mean TSk of the Achilles tendon

Figure 2
An image obtained from the FLIR ONE with anatomical markers
1. Calcaneal marker
2. Medial Mallelous marker
3. Lateral Malleolus marker
4. Muscle tendon junction marker

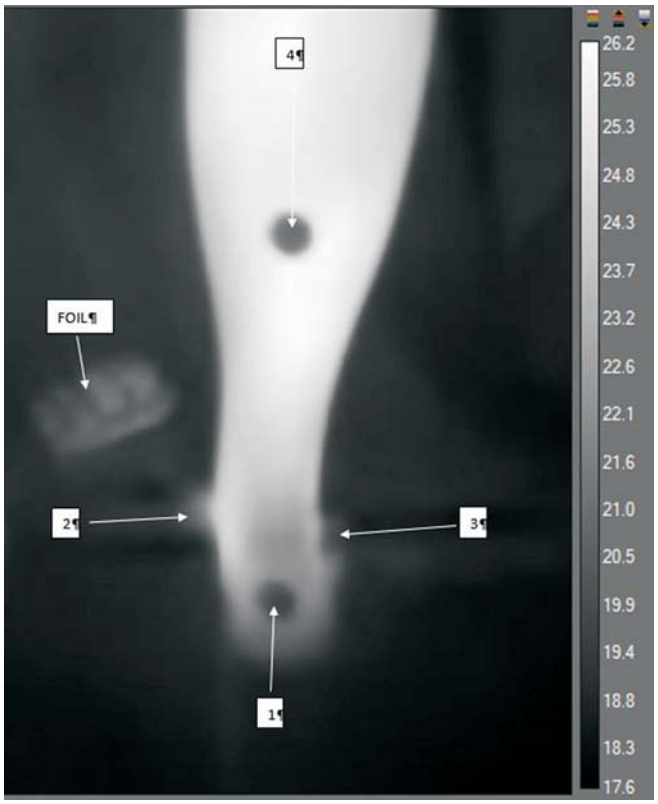

Figure 3
An image obtained from the FLIR E8 identifying anatomical markers
1. Calcaneal marker
2. Medial Mallelous marker
3. Lateral Malleolus marker
4. Muscle tendon junction marker

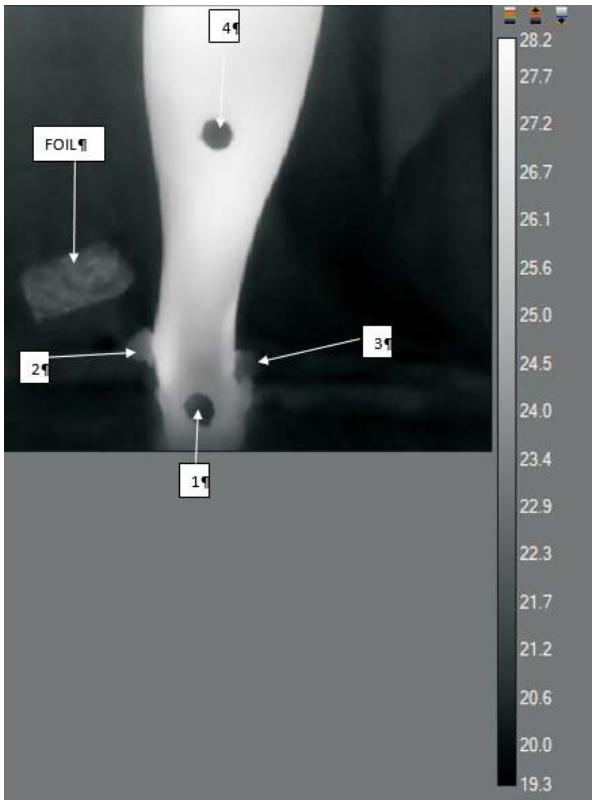

then began from the data point equating to 2cm proximal to the insertion. The number of pixels that equated to a 6cm distance was followed from here, so that the TSk could be tracked beyond the midpoint of the AT, to identify ΔT at the proximal midpoint. The mean Achilles tendon TSk was calculated from these points. An example of this image analysis can be seen in figure 4.

This method was repeated after one week to establish intra-rater reliability and one month later by a second-rater to identify inter-rater reliability. Rater one had two years of experience with infrared thermal imaging analysis as part of a PhD project and rater 2 had no prior experience with thermal image analysis.

Statistical analysis

Intra-rater and inter-rater reliability were assessed using SPSS for Windows (v24.0 SPSS Inc, Chicago, Illinois, USA). Assumptions of normality were assessed using the Shapiro-Wilks test. Unless stated differently, data are presented as mean ± standard deviation (SD).

Intraclass correlation coefficient (ICC) two-way mixed-effects, absolute agreement, single measurement model was utilised to assess intra-rater reliability. A two-way random-effects, absolute agreement, single measurement model was used to assess inter-rater reliability, in line with recommendations from Koo and Li (2016) [24]. Values <0.5 were considered poor, 0.5-0.75 was considered moderate, 0.75-0.9 was good and values >0.9 indicated excellent reliability. Once the ICC's were calculated, the means and SD's of rating 1 and rating 2 for both intra-rater and inter-rater reliability, the 95% confidence intervals (CI), the SEM's and MDC's were calculated using Microsoft Excel (v16.0, Micro- soft corporation, WA, US). The SEM was calculated using the equation (SD(pooled)*($\sqrt{1-ICC}$ and the MDC was calculated using the formula (1.96*$\sqrt{2}$)*SEM). Microsoft Excel was used in order to calculated the pooled SD

$$\sqrt{\frac{(SDrating1 * SDrating1) + (SDrating2 * SDrating2)}{2}}.$$

Intra-rater, Inter-rater and between device agreement were assessed using Bland Altman analysis, the mean bias and 95% limits of agreement (LoA) in SPSS. Mean bias represents the mean difference between rating/rater 1 and rating/rater 2 and between the FLIR ONE and FLIR E8. The

Figure 4
An example of the infrared thermal image analysis

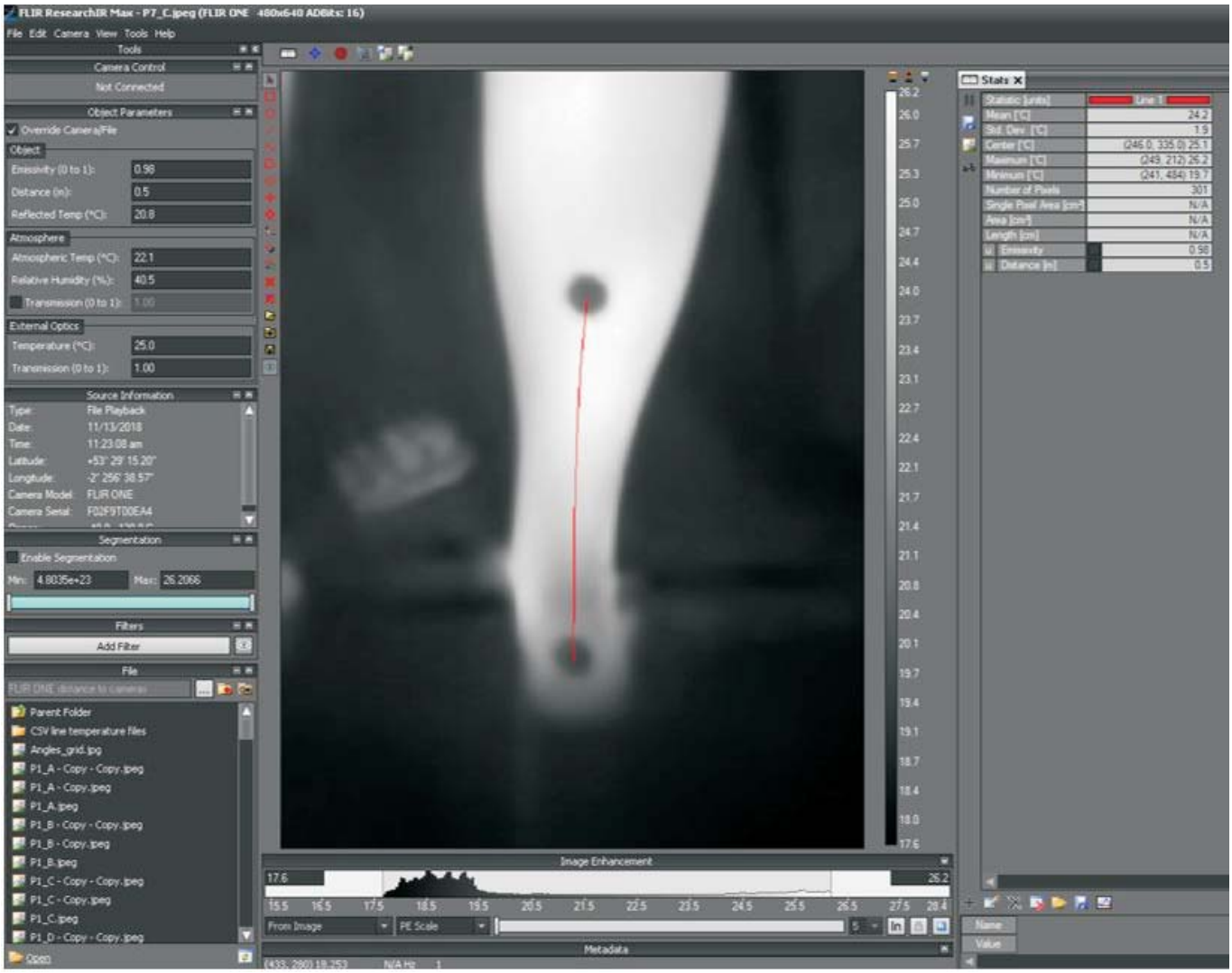

95% LoA represent the range of difference within which we would expect 95% of data points to lie and was calculated using the following equation Bias ±1.96 x SD. The manufacturer stated accuracy of the FLIR ONE is ±5% therefore a priori acceptable mean bias is defined as a value within 5% of the mean TSk measurement to account for measurement error [27] . The manufacturer stated accuracy of the FLIR E8 is ±2% therefore a priori acceptable mean bias is defined as a value within 2% of the mean TSk measurement to account for measurement error [27].

Table 3
Mean, SD and 95% CI's for the TSk data from the FLIR ONE and FLIR E8 at 0.5m and 1m

Camera	Distance (m)	Mean Tsk (°C)	SD (°C)	95% CI	
FLIR ONE	0.5	27.7	1.8	26.8	28.6
	1	27.7	1.2	27.1	28.4
FLIR E8	0.5	26.6	1.2	26.0	27.2
	1	26.3	1.4	25.6	27.1

Table 4
Intra-rater reliability ICC, 95% CI's, SEM's and SDD's for the FLIR ONE and FLIR E8 at 0.5m and 1m

Camera	Distance (m)	ICC	95% CI		SEM (°C)	MDC (°C)
FLIR ONE	0.5	0.99	0.96	1.00	0.2	0.5
	1	0.99	0.96	1.00	0.1	0.4
FLIR E8	0.5	0.98	0.81	1.00	0.2	0.5
	1	0.95	0.27	0.99	0.3	0.9

Figure 5
Bland Altman plots for intra-rater agreement for the FLIR ONE

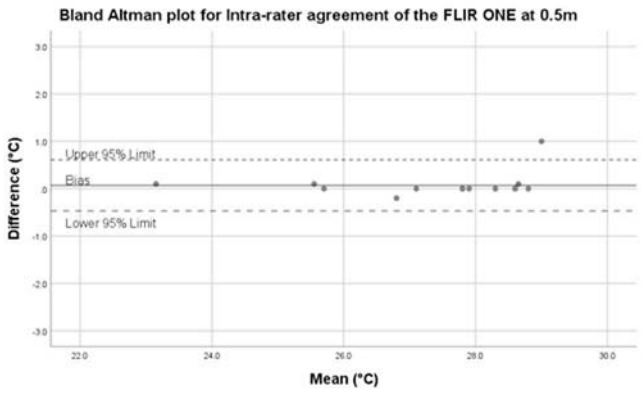

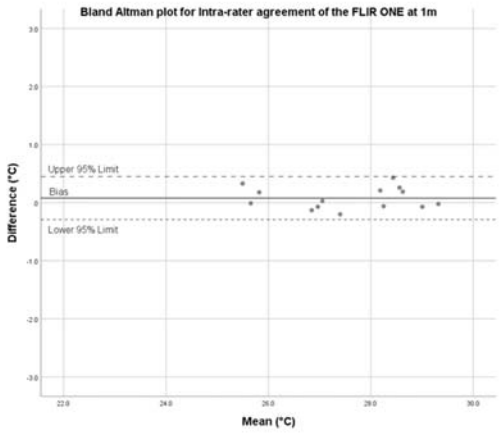

Figure 6
Bland Altman plots for intra rater agreement of the FLIR E8

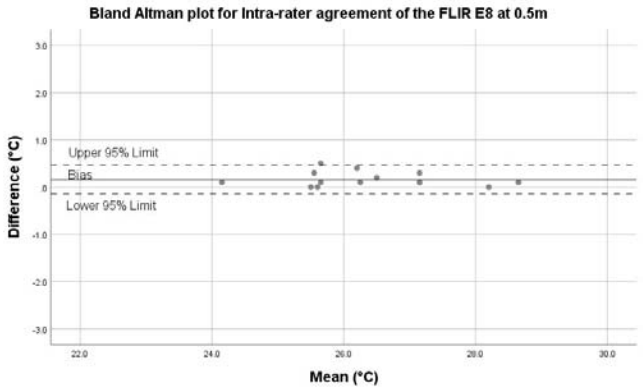

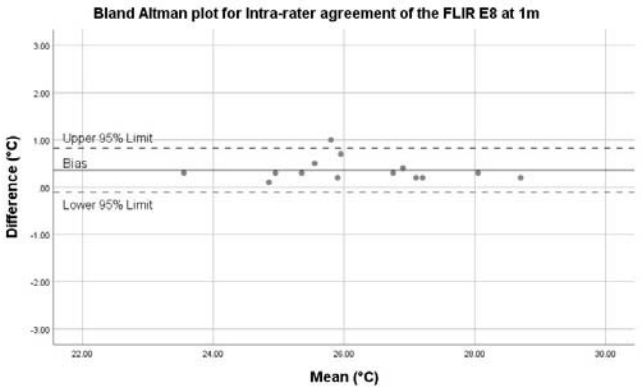

Results

Assumptions of normality were not violated (p>0.05). The mean TSk values, SD's and 95% CI's can be seen in table 3 for both cameras.

Intra-rater reliability

The method used to analyse TSk of the midportion of the Achilles tendon demonstrated excellent intra-rater reliability at both 0.5m and 1m distances from the ROI for images captured by both the FLIR ONE and the FLIR E8. The ICC's, 95% CI's, SEM's and MDC's can be seen in table 4. Mean bias and LoA can be seen in table 5. Bland Altman plots can be seen in figures 5 and 6.

Table 5
Intra-rater agreement of the FLIR ONE and FLIR E8

Device	Distance (m)	Bias (°C)	Lower 95% LoA (°C)	Upper 95% LoA(°C)
FLIR ONE	0.5	0.07	-0.47	0.61
	1	0.08	-0.29	0.45
FLIR E8	0.5	0.16	-0.14	0.47
	1	0.36	-0.11	0.82

Inter-rater reliability

There was excellent inter-rater reliability for the method used to analyse TSk of the midportion of the Achilles tendon for data captured by the FLIR ONE at a distance of 0.5m and for the values obtained by the FLIR E8 at 0.5m and 1m distances. At a 1m distance, this inter-rater reliability was classed as good for data captured by the FLIR ONE. These results can be seen in table 6. Mean bias and LoA can be seen in table 7. Bland Altman plots can be seen in figures 7 and 8.

Table 6
Inter-rater reliability ICC, 95% CI's, SEM's and SDD's for the FLIR ONE and FLIR E8 at 0.5m and 1m

Device	Distance (m)	Bias (°C)	95% CI		SEM (°C)	MDC (°C)
FLIR ONE	0.5	0.97	0.54	0.99	0.3	0.9
	1	0.79	0.48	0.93	0.6	1.6
FLIR E8	0.5	0.97	0.61	0.99	0.2	0.6
	1	0.99	0.97	1.00	0.1	0.4

Inter-device agreement

Agreement between the two infrared thermal imaging cameras was not acceptable. Mean bias and the 95% LoA were high at both 0.5m and 1m distances and the confidence limit exceeded the a priori acceptable figures, as can be seen in table 8 and figure 9.

Table 7
Inter-rater agreement of the FLIR ONE and FLIR E8

Device	Distance (m)	Bias (°C)	Lower 95% LoA (°C)	Upper 95% LoA(°C)
FLIR ONE	0.5	-0.36	-0.92	0.21
	1	-0.28	-1.80	1.25
FLIR E8	0.5	-0.23	-0.62	0.15
	1	0.04	-0.33	0.40

Figure 7
Bland Altman plots for interrater agreement of the FLIR ONE

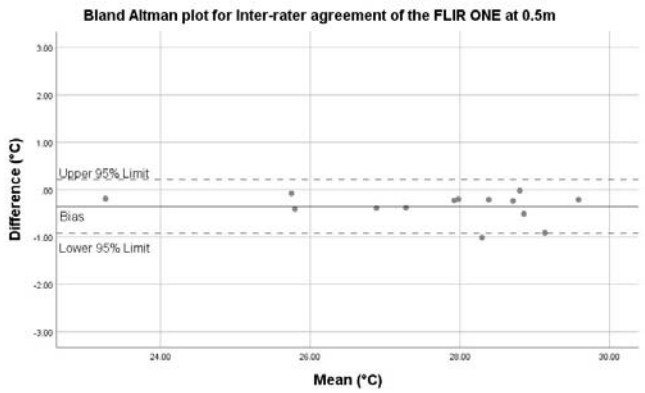

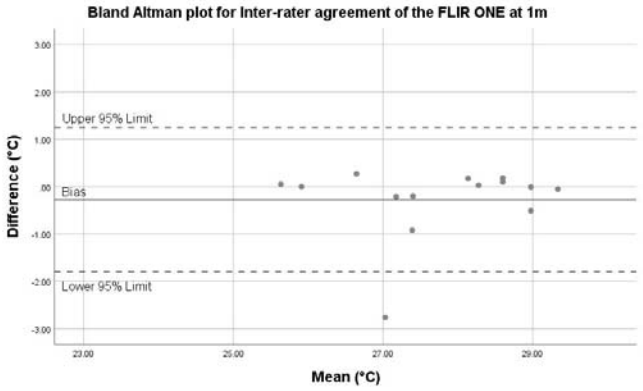

Figure 8
Bland Altman plots for inter-rater agreement of the FLIR E8

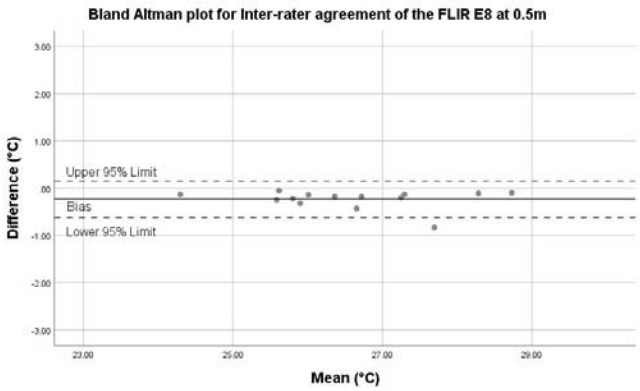

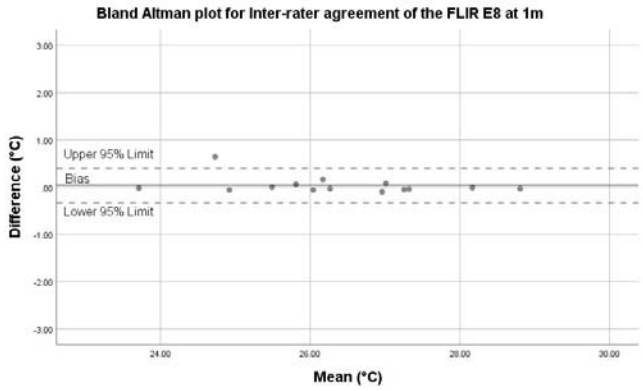

Discussion

The aim of this study was to establish the intra-rater and inter-rater reliability of a method of analysing the TSk of the midportion of the Achilles tendon.

There was excellent intra-rater reliability of the method used to analyse Achilles tendon TSk at a distance of 0.5m with data captured from as seen in table 4. The results revealed a low SEM (0.2°C) and a low MDC (0.5°C). There was also excellent intra-rater reliability at a 1m distance with the data obtained from the FLIR ONE, with a low SEM (0.1°C) and a low MDC (0.4°C). In comparison, despite also having excellent intra-rater reliability at both distances, the SEM and MDC values for the FLIR E8 were higher than those from the FLIR ONE. The higher SEM's and MDC's obtained from the FLIR E8 suggest that the methodology used results in more reliable readings from the FLIR ONE possibly due to the interpolation of images creating a temperature point every 4x4 pixels, meaning that despite more pixels being available with the analysis image, there is only TSk change every 4 pixels in each direction. It also suggests that the consistency of line placement by rater one is excellent. However, this same reason could also explain why there are lower SEM's and MDC's from the FLIR E8 during inter-rater interpretation of the images, with 230,400 ((480x640) - (320x240)) more pixels being available in the FLIR ONE image there is a greater chance for variation in line placement throughout the midportion of the Achilles when rater 2 analysed images compared to rater 1, despite temperature change only occurring every 4x4 pixels.

As the distance increases from 0.5m to 1m, the clarity of the thermal image decreases, making it harder to identify the borders of the Achilles tendon, as seen in figure 10. Less pixels cover the ROI on the tendon, which may explain why the inter rater ICC is low, and the SEM and MDC values are higher.

Tumilty et al. [28] also assessed the Achilles tendon using an infrared thermal imaging camera. Their study focussed on assessing the TSk of the Achilles over a 9-week period of a collegiate cross-country season. The infrared thermal camera that they used was the FLIR T450SC, which was similar to that of the FLIR E8, with a 320x240 infrared thermal pixel count, a 1% accuracy and a sensitivity <0.05°C. Interestingly, the emissivity value was set to 0.95, but the recommended emissivity setting of human skin is 0.98 [29].

Whilst the study displayed acceptable ICC's, the methodology used would not be appropriate for measuring changes in Achilles tendon TSk in response to exercise, which may limit the usability of thermography in the athletic setting. Tumilty et al. (2019) utilised the box analysis tool in the FLIR Tools (FLIR Systems, Oregon, US) software programme. They standardised the analysis by using a 10x40 ROI. The distal border of the box was defined as the point on the calcaneus where there was a colour change between the bone and the tendon as judged by the rater. It may have been possible that the colour change was different between sessions and between participants, meaning that TSk may be read from different locations. Additionally, if this was to be used as a tool for tracking TSk post-exercise, there may be substantial changes in the thermal profiles around the calcaneus, meaning that it may not be possible to standardise box placement using colours alone. Additionally, not all Achilles tendons travel in a linear fashion, meaning that a

Figure 10
An image obtained by the FLIR ONE at 0.5m (A) and an image of the same tendon from

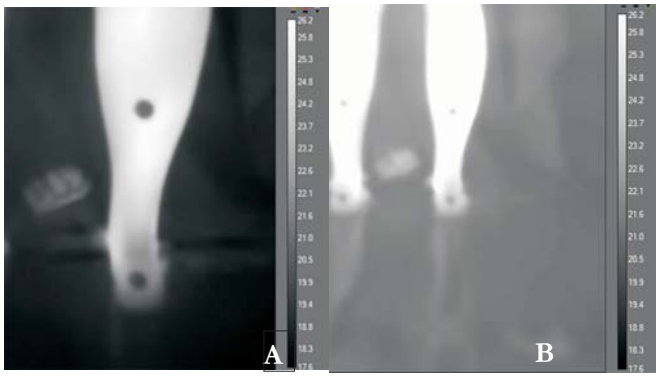

Figure 9
Bland Altman plots for inter-device agreement FLIR ONE versus FLIR E8

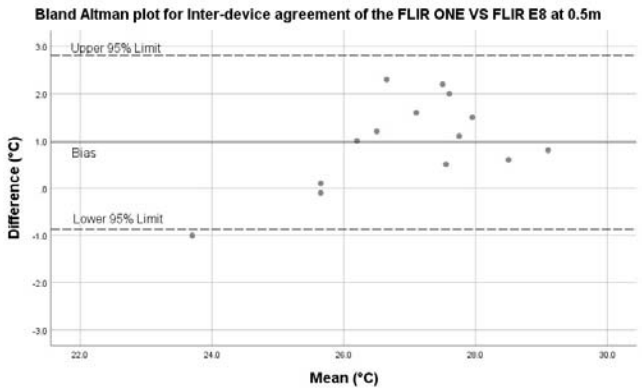

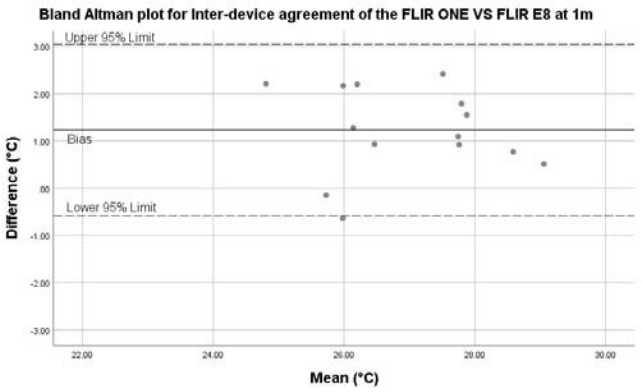

box placement may encompass areas medial and lateral to the tendon. In close proximity to the Achilles tendon medially, lies the Posterior Tibial Artery [30], which could impact TSk readings when a box tool is used. The results highlight the need for identification of known anatomical landmarks opposed to a post-hoc placement of ROI's based on temperature profiles.

In agreement with the hypothesis, the FLIR ONE had excellent inter-rater reliability at a 0.5m distance, with low SEM's (0.3°C) and MDC's (0.9°C). The inter-rater reliability at 1m was good, with a slightly higher SEM (0.6°C) and MDC (1.6°C). In comparison, the FLIR E8 had excellent inter-rater reliability at both 0.5m (SEM 0.2°C, MDC 0.6°C) and 1m distances (SEM 0.1°C, MDC 0.4°C).

The FLIR E8 has lower SEM's that the FLIR ONE at both 0.5m and 1m distances from the ROI when analysed between clinicians. The cost of the two devices to purchase is vast, with the FLIR ONE retailing at approximately one-tenth of that of the FLIR E8. This difference in price, combined with the acceptable intra-rater and inter-rater reliability may mean that clinically, infrared thermography may now be a viable option to track Achilles tendon TSk. It is important to note that the results of this study do not infer that the devices can track TSk change over time, which could be useful future study. Based upon these results, it is suggested that measures of TSk using the FLIR ONE infrared thermal imaging camera are taken from a distance of 0.5m in order to improve the reliability of the readings. The results of the current study also reveal that the inter-device agreement is unacceptable, with mean bias and 95% LoA lying outside the acceptable 2% limits as defined a priori. It is therefore recommended that despite high reliability of the TSk analysis method of the FLIR ONE and the FLIR E8, when absolute TSk values are used, results between the devices are not compared, as the devices do not agree sufficiently.

At a distance of 0.5m the MDC for the FLIR ONE between raters of vastly different experience levels is 0.9°C, and 1.6°C at a distance of 1m. For the assessment of Achilles tendon TSk, it is not known whether these are acceptable and further work beyond the reliability of method analysis is required. ΔT between the symptomatic and asymptomatic Achilles tendon is expected to exceed this in response to loading exercise based on early preliminary experimentation. Future study will investigate what the normal TSk response of symptomatic vs asymptomatic Achilles tendons is and whether an MDC of 1.6°C is excessively large.

Limitations

A limitation in the methodology was identified; in the tallest participant, who measured 184.2cm in height, the most proximal anatomical marker was not fully visible. It is anticipated that taller participants may undergo data collection in the future, therefore it may be appropriate to move the camera backwards in relation to the ROI to account for this. It is therefore recommended that for future study, the effect of distance on TSk readings over the midportion of the Achilles tendon is assessed, to see whether moving the camera results in statistically significant ΔT.

This study did not assess the repeatability of the device over time. Future study will assess this.

Conclusion

The method of analysis used for the FLIR ONE infrared thermal imaging camera displayed acceptable intra-rater and inter-rater reliability for use in the assessment of Achilles tendon TSk. At a 0.5m distance, a ΔT of 0.5°C would be classed as significant change that we can be sure is not due to error when comparing intra-rater readings, and a ΔT of 1.2°C would be the value when comparing between two raters of vastly different experience levels. At 1m 0.4°C would be classed as significant TSk change that we can be sure is not due to error when assessed intra-rater and a ΔT of 1.6°C would be the value when comparing between two raters of differing experience. Caution must be drawn in future study if the camera is moved between 0.5m and 1m distances, and new ICC, SEM and MDC values must be calculated to ensure robust results. The absolute TSk values should not be used interchangeably between the FLIR ONE and the FLIR E8 as the results from the analysis method show that the devices do not agree sufficiently.

Conflict of interest

The authors declare that there are no conflicts of interest.

References

1. O'Neill S. A biomechanical approach to Achilles tendinopathy management [Doctoral Dissertation]: University of Leicester; 2016

2. Gajhede-Knudsen M, Ekstrand J, Magnusson H, Maffulli N. Recurrence of Achilles tendon injuries in elite male football players is more common after early return to play: An 11-year follow-up of the UEFA Champions League injury study. Br. J. Sports Med. 2013;47:763-8.

3. Sankey RA, Brooks JHM, Kemp SPT, Haddad FS. The epidemiology of ankle injuries in professional rugby union players. Am. J. Sports Med. 2008;36:2415-24.

4. De Jonge S, Van Den Berg C, De Vos RJ, Van Der Heide HJL, Weir A, Verhaar JAN, et al. Incidence of midportion Achilles tendinopathy in the general population. Br. J. Sports Med. 2011;45:1026-8.

5. D'Addona A, Maffulli N, Formisano S, Rosa D. Inflammation in tendinopathy. Surgeon. Elsevier Ltd; 2017;15:297-302.

6. Kragsnaes MS, Fredberg U, Stribolt K, Kjaer SG, Bendix K, Ellingsen T. Stereological quantification of immune-competent cells in baseline biopsy specimens from achilles tendons: Results from patients with chronic tendinopathy followed for more than 4 years. Am. J. Sports Med. 2014;42:2435-45.

7. Maffulli N, Sharma P, Luscombe KL. Achilles tendinopathy: aetiology and management. Jrsm. 2004;97:472-6.

8. Bramah C, Preece SJ, Gill N, Herrington L. Is There a Pathological Gait Associated With Common Soft Tissue Running Injuries? Am. J. Sports Med. 2018;46:3023-31.

9. Debenham J, Travers M, Gibson W, Campbell A, Allison G. Eccentric Fatigue Modulates Stretch-shortening Cycle Effectiveness - A Possible Role in Lower Limb Overuse Injuries. Int. J. Sports Med. 2015;37:50-5.

10. Wang HK, Lin KH, Su SC, Shih TTF, Huang YC. Effects of tendon viscoelasticity in Achilles tendinosis on explosive performance and clinical severity in athletes. Scand. J. Med. Sci. Sport. 2012;22:1-9.

11. Turner T, Pansch J, Wilson J. Thermographic assessment of racing Thoroughbreds. 47th Annu Conv Am …. 2001;47:344-6.

12. Fernández-Cuevas I, Marins JC, Carmona PG, García- Concepción MA, Lastras JA, Quintana MS. Reliability and reproducibility of skin temperature of overweight subjects by an Infrared Thermography software designed for human beings. Thermol. Int. 2012;22(S):S130-S137.

13. Hildebrandt C, Raschner C, Ammer K. An overview of recent application of medical infrared thermography in sports medicine in Austria. Sensors. 2010;10:4700-15.

14. Fernandes AA, Moreira DG, Brito CJ, da Silva CD, Sillero-Quintana M, Pimenta EM, et al. Validity of inner canthus temperature recorded by infrared thermography as a non-invasive surrogate measure for core temperature at rest, during exercise and recovery. J. Therm. Biol. 2016;62:50-5.

15. Bach AJE, Stewart IB, Disher AE, Costello JT. A Comparison between Conductive and Infrared Devices for Measuring Mean Skin Temperature at Rest , during Exercise in the Heat , and Recovery. 2015;10:1-13.

16. McFarlin BK, Venable AS, Williams RR, Jackson AW. Comparison of techniques for the measurement of skin temperature during exercise in a hot, humid environment. Biol. Sport. 2015; 32:11-4.

17. Priego Quesada JI, Martínez Guillamón N, De Anda RMCO, Psikuta A, Annaheim S, Rossi RM, et al. Effect of perspiration on skin temperature measurements by infrared thermography and contact thermometry during aerobic cycling. Infrared Phys. Technol. 2015;72:68-76.

18. Kanazawa T, Nakagami G, Goto T, Noguchi H, Oe M, Miyagaki T, et al. Use of smartphone attached mobile thermography assessing subclinical inflammation: a pilot study. J. Wound Care. 2016;25:177-82.

19. Wilkinson JD, Leggett SA, Marjanovic EJ, Moore TL, Anderson ME, Britton J, et al. A Multicenter Study of the Validity and Reliability of Responses to Hand Cold Challenge as Measured by Laser Speckle Contrast Imaging and Thermography Outcome Measures for Systemic Sclerosis - Related Raynaud ' s Phenomenon. Arthritis Rheumatol. 2018;70:903-11.

20. Langemo DK, Spahn JG. A Reliability Study Using a Long-Wave Infrared Thermography Device to Identify Relative Tissue Temperature Variations of the Body Surface and Underlying Tissue. Adv. Skin Wound Care. 2017;30:109-19.

21. Cao J, Currie K, Carry P, Maddox G, Nino S. Smartphone-Based Thermal Imaging?: A New Modality for Tissue Temperature Measurement in Hand and Upper Extremity Surgeries. Hand. 2018;13:350-4.

22. Jaspers MEH, Carrière ME, Meij-de Vries A, Klaessens JHGM, van Zuijlen PPM. The FLIR ONE thermal imager for the assessment of burn wounds: Reliability and validity study. Burns. 2017;43:1516-23.

23. Mandrekar JN. Measures of interrater agreement. J. Thorac. Oncol. Elsevier; 2011;6:6-7.

24. Koo TK, Li MY. A Guideline of Selecting and Reporting Intraclass Correlation Coefficients for Reliability Research. J. Chiropr. Med. Elsevier B.V.; 2016;15:155-63.

25. Moreira DG, Costello JT, Brito CJ, Adamczyk JG, Ammer K, Bach AJE, et al. Thermographic imaging in sports and exercise medicine: A Delphi study and consensus statement on the measurement of human skin temperature. J. Therm. Biol. 2017; 69:155-62.

26. Bujang MA, Baharum N. A simplified guide to determination of sample size requirements for estimating the value of intraclass correlation coefficient: A review. Arch. Orofac. Sci. 2017; 12: 1-11

27. Hanneman SK. Design, analysis, and interpretation of method-comparison studies. AACN Adv. Crit. Care. 2008;19:223-34.

28. Tumilty S, Adhia DB, Smoliga JM, Gisselman AS. Thermal profiles over the Achilles tendon in a cohort of non-injured collegiate athletes over the course of a cross country season. Phys. Ther. Sport. Elsevier Ltd; 2019;36:110-5.

29. Fernández-Cuevas I, Bouzas Marins JC, Arnáiz Lastras J, Gómez Carmona PM, Piñonosa Cano S, García-Concepción MÁ, et al. Classification of factors influencing the use of infrared thermography in humans: A review. Infrared Phys. Technol. 2015;71:28-55.

30. Chen TM, Rozen WM, Pan W, Ashton MW, Richardson MD, Taylor GI. The arterial anatomy of the Achilles tendon: Anatomical study and clinical implications. Clin. Anat. 2009; 22: 377-85.

Address for Correspondence

Ben Oliver

Salford University School of Health and Society

Salford M6 6PU,

United Kingdom

Email: b.oliver1@edu.salford.ac.uk

(Received 08.2019, revision accepted 07.11.2019)

A case study on dynamic thermal imaging evaluation of a thyroid nodule

R. Vardasca[1,2,4,] C. Magalhaes[1,2], C. Freitas[3], J. Mendes[1,2]

[1]Faculdade de Engenharia, Universidade do Porto, Porto, Portugal
[2]LABIOMEP, INEGI, Porto, Portugal
[3]Endocrinology department, Centro Universitário e Hospitalar do Porto, Porto, Portugal
[4]Faculty of Computing, Engineering and Science, University of South Wales, Pontypridd, United Kingdom

SUMMARY

BACKGROUND:The thyroid gland is a butterfly-shaped organ located in the neck anteriorly to the larynx and trachea, typically extending from the level of C5-T1. It is responsible for the release of hormones that control metabolic rates and thereby modifying obligatory and adaptive thermogenesis. This organ can be affected by nodules and cellular malformations, which can result in malignant neoplasia or benign cysts. Those manifestations may change the normal pattern of skin temperature distribution in the affected area. The aim of this study is to investigate the thermal pattern of a subject presenting a hypervascularized nodule located on the left side of the thyroid.

MATERIALS AND METHODS: A male with 40 years old presenting a 11x6 mm nodule in the left side of his thyroid, confirmed by functional doppler imaging, was examined in a controlled environment using a FLIR E60 thermal camera and two aluminium disks to provide a cooling provocation during one minute on the skin, above the thyroid gland location. Thermal images were taken before and until the fifth minute after cooling at an interval of 1 minute. A 26x26 pixel square region of interest (ROI) was drawn in the analysis software to statistically analyze the temperature values, histogram, mean, median and mode temperature, standard deviation, kurtosis and skewness per ROI and side.

RESULTS:The ROI presented at baseline a bilateral difference in mean temperature of 0.4 ºC, after cooling this difference was accentuated, the affected side recovered quickly and showed a hot spot in the area of the nodule identified by Doppler imaging.

CONCLUSION:This case study showed evidence of the utility on using dynamic infrared thermal imaging when assessing thyroid nodules, which was confirmed by Doppler imaging to be highly vascularized. However, for diagnostic purposes the traditional expensive methods such as biopsy and nuclear medicine are still required. Still the application of IRT imaging should be further researched in possible monitoring and documenting the diagnosis and treatment evaluation applied to thyroid conditions.

KEY WORDS: Dynamic thermography; skin temperature; thermal symmetry; thyroid nodule

EINE FALLSTUDIE ZUR AUSWERTUNG EINES DYNAMISCHEN WÄRMEBILDES EINES SCHILDDRÜSENKNOTENS

HINTERGRUND: Die Schilddrüse ist ein schmetterlingsförmiges Organ, das sich am Hals vor dem Kehlkopf und der Luftröhre befindet und sich typischerweise auf Höhe C5-T1 erstreckt. Es ist für die Freisetzung von Hormonen verantwortlich, die Stoffwechselraten steuern und damit die obligatorische und adaptive Thermogenese verändern. Dieses Organ kann durch Knötchen und zelluläre Fehlbildungen verändert werden, die zu bösartiger Neoplasie oder gutartigen Zysten führen können. Diese Manifestationen können das normale Muster der Hauttemperaturverteilung im betroffenen Bereich verändern. Ziel dieser Studie ist es, das thermische Muster einer Person zu untersuchen, die ein hyper-vaskularisiertes Knötchen auf der linken Seite der Schilddrüse aufweist.

METHODE: Ein durch funktionelle Doppler-Bildgebung bestätigter 11x6-mm großen Knoten an der linken Seite der Schilddrüse eines 40 Jahre alten Mannes, , wurde in einer kontrollierten Umgebung mit einer FLIR E60-Wärmebildkamera untersucht, nachdem mit zwei Aluminiumscheiben die Haut über der Schilddrüsen 1 Minute lang gekühlt worden war. Wärmebilder wurden vor und bis zur fünften Minute nach der Kühlung im Minutenabstand aufgenommen. Mit der Analysesoftware wurde ein quadratischer 26x26 Pixel großer Auswertebereich (ROI) gezeichnet, um Temperaturwerte, Histogramm, Mittelwert, Median- und Modus-Wert der Temperatur, Standardabweichung, Kurtose und Schiefe pro ROI und Seite statistisch zu analysieren.

ERGEBNISSE: Zu Beginn fand sich ein Seitenunterschied der mittleren Temperatur von 0,4°C. Dieser Unterschied verstärkte nach der Kühlung, die betroffene Seite erholte sich rasch und zeigte einen Hot Spot in dem Bereich, der durch Doppler-Bildgebung als Knötchen identifiziert worden war.

SCHLUSSFOLGERUNG: Diese Fallstudie liefert Hinweise für den Nutzen der dynamischen Infrarot-Thermographie bei der Beurteilung von Schilddrüsenknoten, die durch Doppler-Bildgebung als hoch vaskularisiert bestätigt wurde. Trotzdem sind für diagnostische Zwecke die traditionellen kostspieligen Methoden wie Biopsie und Nuklearmedizin weiterhin erforderlich. Dennoch sollte die Anwendung der Infrarot-Bildgebung für eine mögliche Überwachung und Dokumentation der Diagnose und Behandlungsbewertung von Schilddrüsenerkrankungen weiter erforscht werden.

SCHLÜSELWÖRTER: Dynamische Thermographie; Hauttemperatur; thermische Symmetrie; Schilddrüsenknoten

Thermology international 2019, 29(4) 146-153

Introduction

The thyroid gland is a large endocrine gland located in the neck anteriorly to the larynx and trachea, typically extending from the level of C5- T1. Thyroid hormone influences the metabolic rate in all cells of the body and modifies many other metabolic processes in a complex interaction with other hormones. By governing the metabolism, the thyroid gland is contributing to the human homeostasis and heat production [1].

This organ can develop cellular malformations, which can result in nodules that can be benign or malignant. In case of carcinoma, it is one type of cancer that has grown in incidence over the last decade, especially in women and at an early age (2). It has a relatively low mortality rate but has a high number of recurrences (3, 4). The most common method of diagnosis is through biopsy and nuclear medicine. The common treatments available today are surgery and radiation, the surgery can be total (thyroidectomy) or partial (ablation), the radiation can be through iodine I131 or chemotherapy (5). The fact that this neoplasm is not associated with a high mortality rate lea to high treatment costs (6). The total surgery in addition to the costs of the procedure is linked to the dependency of drugs and additional costs for the lifetime (4).

Infrared thermal (IRT) imaging has already been used for designing with success a prototype of a model to aid the diagnose of thyroid gland disease (7), however advanced image processing methods and the use of dynamic thermography could improve it. The idea of using the IRT technique in the research of thyroid conditions is not new, the first suggestions were made in the 1970's (8,9), where the authors described the method as an extremely valuable new technique for the evaluation of thyroid nodules to aid the diagnosis and follow up, since it is harmless to the patients.

Other conditions that affect this gland, such as hyperthyroidism causes an increase of cutaneous temperature. Combining IRT imaging and isotope scanning was useful for investigating non-active thyroid nodules; while malignant tumors tend to present an increase in cutaneous temperature, cysts could give rise to areas of relative hypothermia. An increase in temperature was also showed in I131 active toxic adenomas (10).

Clack et al. (11) when correlating the finding of ultrasonography and IRT examination have found that there was a good correspondence between the two imaging methods but without clinical significance.

Another research (12) found no evident correlation between the thermal gradient and the clinical diameter of the thyroid nodule, the authors stated that thermography is not reliable when used to select cold thyroid nodules for surgical removal.

Helmy et al. (7) assessed the IRT potential in the detection of thyroid nodules. A cube was used as a simple geometric shape model for the neck and performed a thermal analysis based in the thyroid gland being a heat source. Finite Element Analysis was used and it was concluded that the results of the new diagnostic method were in good agreement with the current existing diagnostic method. However, this is a theoretical model and was never implemented in practice

Figure 1
Location of the thyroid gland and nodule.

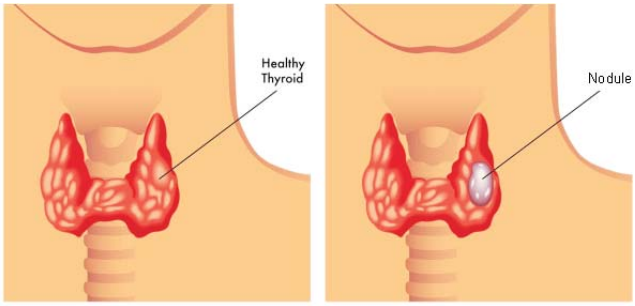

A study in Nigeria (14) concluded that IRT could be relevant, and if combined with other imaging modality could play a relevant role in the differential diagnosis of thyroid diseases, providing more complementary data in evaluation of the thyroid.

Another research using MRI and IRT imaging (14) demonstrated that thermal contributions caused by varying the breathing frequency and blood-flow velocity are negligibly small enforcing the value of using IRT in investigations of thyroid diseases.

Alves and Gabarra (15) compared the two imaging methods of IRT and power Doppler sonography in the detection of thyroid nodules, results demonstrated higher accuracy and precision of IRT in the diagnosis of thyroid nodules.

Other authors (14, 16, 17) suggest that IRT can detect thermal differences of skin overlying the thyroid, which might help to discriminate different thyroid pathological conditions.

González et al. (18) screened the neck of patients with thyroid cancer with IRT images and concluded that the method could be used as non-invasive tool for the detection of thyroid tumors. This was due to the assumed higher metabolic activity of the thyroid tumor in comparison to the healthy tissue, being the nodule detection made through the appearance of hot spots on the thermogram, which disrupts the thermal symmetry of corresponding bilateral areas.

Recent studies (19, 20) have suggested that the use of machine learning classifiers over the findings of thermal images would facilitate the diagnosis of thyroid nodules and cancer. Another research on image processing on a set of thermograms sequence (21), found that the rate of change of temperature, for every pixel within the image was of major importance. The derivation of the temperature for each pixel not only quantifies the overall rate of change of temperature associated with that pixel, but it can remove the dc offset (a non-uniformity caused by the imperfection of individual detectors and readout circuit, which is a characteristic of the technological process of recording an image) component and noise due to its intrinsic averaging func-

tion. Such algorithm would not be computationally demanding and can always guarantee convergence because only one nonlinear variable needs to be optimized, all remaining parameters being linear in nature. This processing was applied to thermal images of the neck of patients with thyroid cancer and this variation rate showed to be more adequate than mean temperatures of regions of interest.

Figure 2
The active Doppler image showing the hyper-vascularised thyroid nodule in the left lobe.

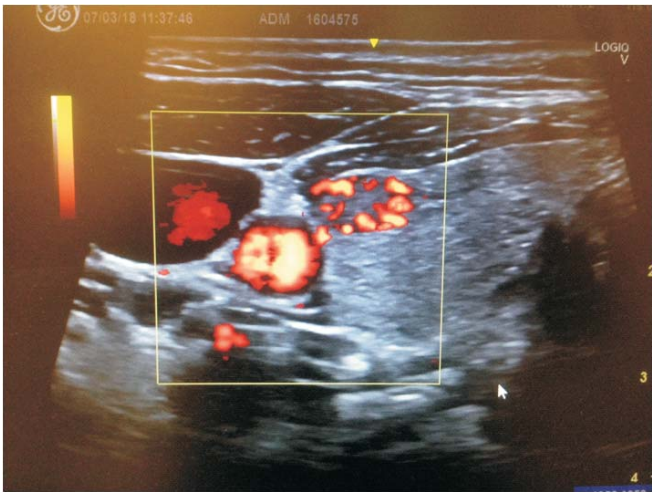

Figure 3
– The aluminum disk used for the thermal provocation over the thyroid area (diameter of 50 mm, thickness of 15 mm)

The aim of this study is to investigate the thermal pattern of a single case of a subject presenting a hypervascularized nodule located on the left side of the thyroid, through different forms of objective image analysis.

Materials and Methods

A male patient with 40 years old and a BMI of 29.7 kg/m2, was identified to have a thyroid nodule of 11x6 mm at the left side of the thyroid gland (figure 1) in an occasional Doppler scan, which also showed a hypervascularization around the nodule as presented in figure 2. The nodule was also identified by palpation.

The study took place, as suggested by IRT imaging recommendations (23-25), in an environmental controlled room of 3 x 4 m in size (with a mean temperature of 22.0 °C, relative humidity of 45%, absence of incandescent lighting over all equipment and laminar low air flow) at the Faculty of Engineering, University of Porto. For image capturing it was used a thermal camera FLIR E60 with a focal plane sensor array size of 320x240, NETD of <50 mK at 30ºC and measurement uncertainty of ±2% of the overall temperature range.

A static thermal image was taken, after the acclimatization period of 15 minutes, from the anterior view of the neck, it was followed by a contact thermal stimulus provided by

Figure 4
Analysis of the images in the FLIR ThermaCAM Researcher Pro 2.10 with the two regions of interest drawn over the thyroid gland. It is clear from the image that the left ROI presents a higher temperature than the right side.

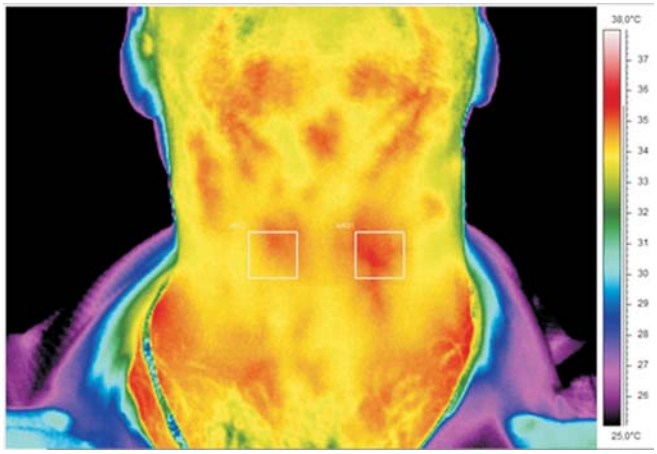

Table 1
The statistical characterization of both ROIs over the provocation test

Time	Right ROI						Left ROI					
	Mean	Median	Mode	sd	Kurtosis	Skewness	Mean	Median	Mode	sd	Kurtosis	Skewness
Baseline	34.5	34.5	34.8	0.3	- 1.23	0.01	34.9	35.0	35.1	0.2	- 0.65	- 0.13
0 min	26.4	26.4	26.4	0.1	- 0.36	0.35	26.8	26.7	26.4	0.4	0.82	0.14
1 min	29.7	29.7	29.7	0.3	0.82	0.38	30.8	30.7	30.1	0.7	- 0.2	0.71
2 min	31.0	31.0	30.9	0.3	- 0.4	0.5	32.3	32.2	32.2	0.2	- 0.48	0.49
3 min	31.7	31.7	31.6	0.3	- 0.32	0.6	32.9	32.8	32.7	0.5	- 0.59	0.31
4 min	31.8	31.7	31.5	0.4	-0.45	0.6	32.6	32.6	32.4	0.6	- 0.32	0.34
5 min	32.1	32.0	31.9	0.3	- 0.72	0.51	33.0	33.0	32.7	0.6	- 0.35	- 0.03

Figure 5
The thermal images taken during the whole dynamic test

Baseline

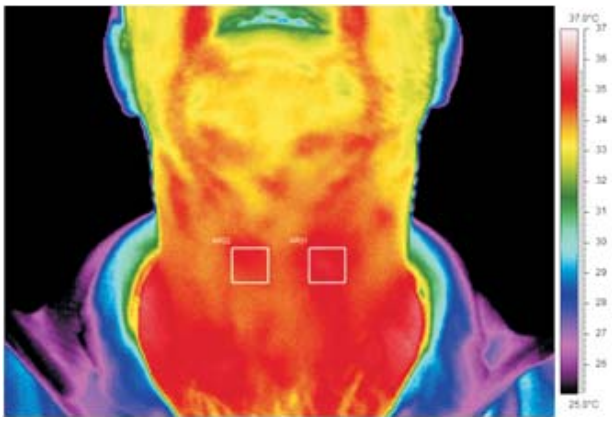

Immediately after provocation

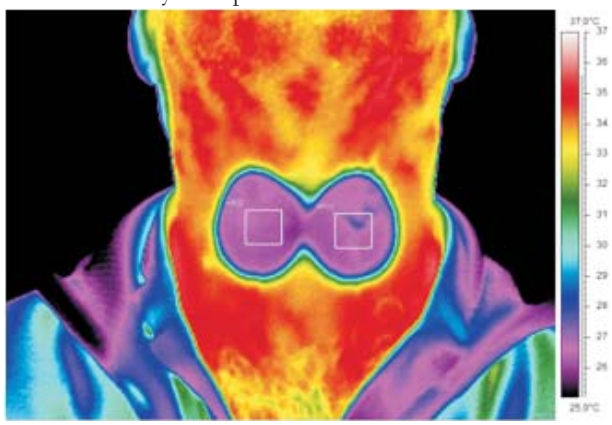

1 minute after provocation

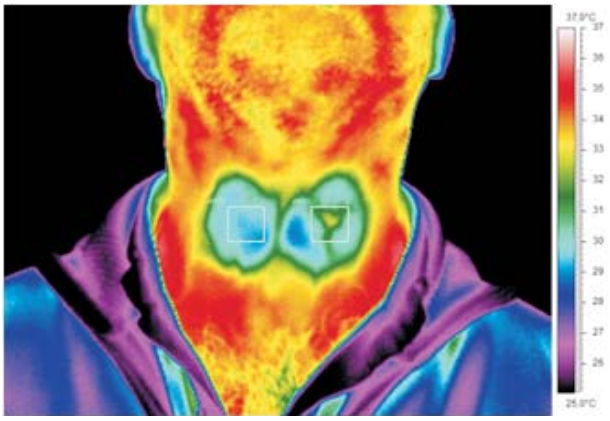

2 minutes after provocation

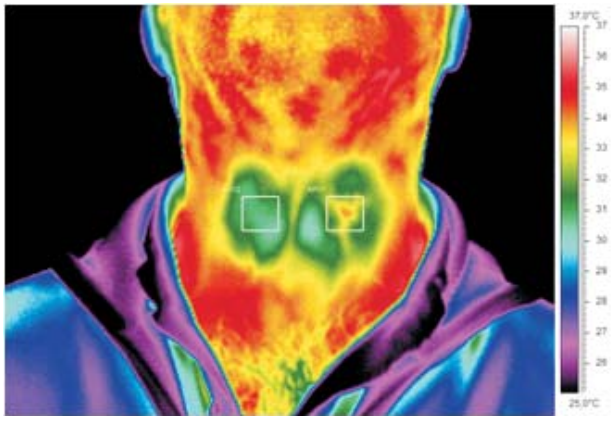

3 minutes after provocation

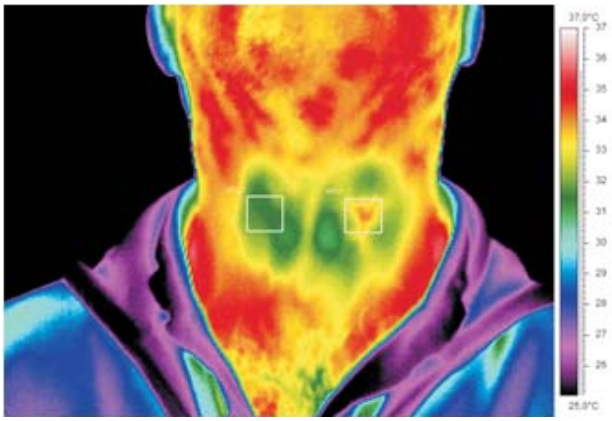

4 minutes after provocation

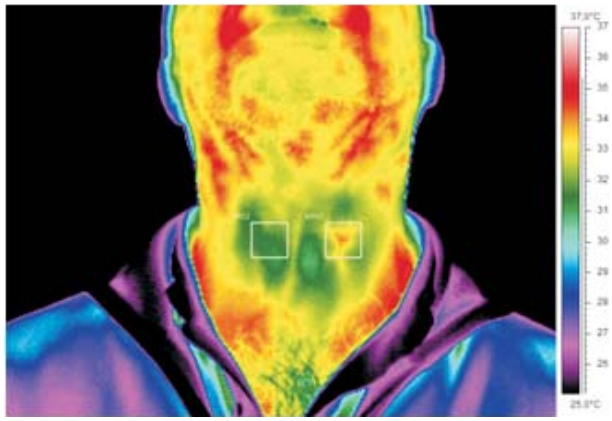

5 minutes after provocation

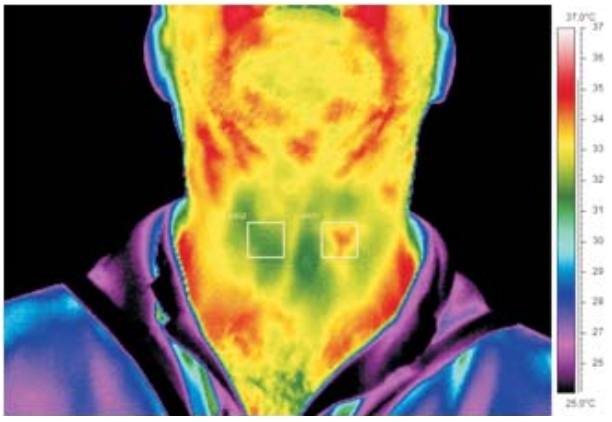

two aluminum disks with 50 mm diameter and 15 mm thick and with a surface temperature equal to examination room environmental temperature, being exposed to it during the whole acclimatization period (figure 3). The disks were applied by conduction during 1 minute on both sides of the anterior neck and above the Adam apple, 5 images were taken at 1-minute interval. Two squared regions of interest (ROI) of 26x26 pixels were drawn at the left and right side of the thyroid skin region using the software package FLIR ThermaCAM Researcher Pro 2.10 for assessing the thermal data, as presented in figure 4.

Figure 6
The histograms of the ROIs over the dynamic test.

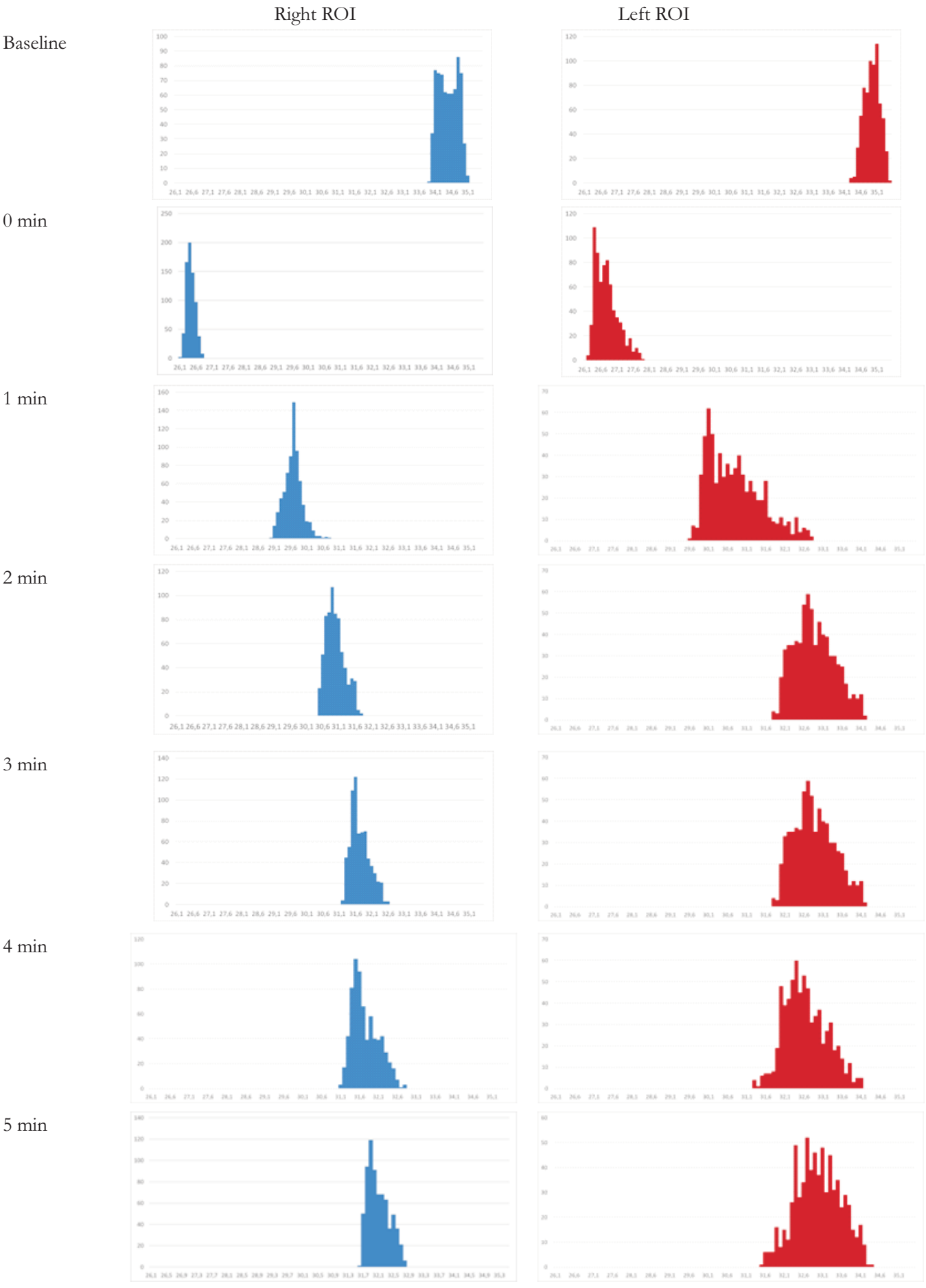

Figure 7
The characteristic charts of statistical parameter for both ROIs over the dynamic assessment.

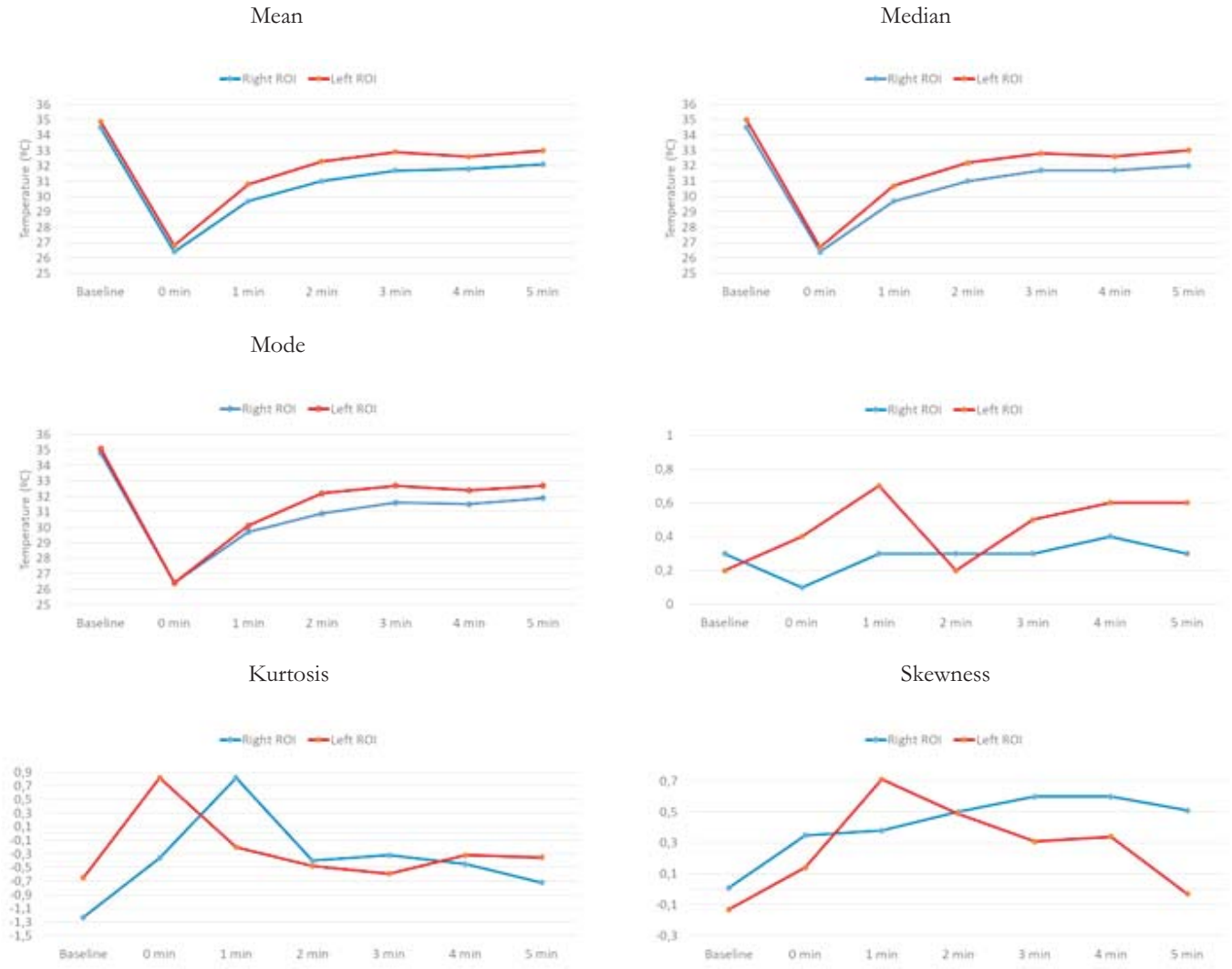

Figure 8
Thermal symmetry between bilateral ROIs along the thermal stimuli test.

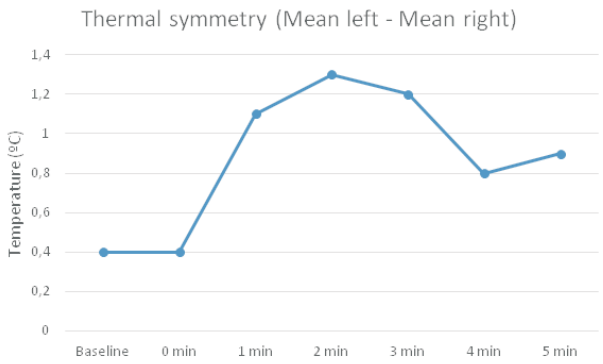

Table 2
The blood test results on the thyroid hormones values

Hormone		Normal Range
Free Thyroxin (Free T4)	1.28 ng/dL	0.93-1.7
Thyrostimulant hormone (TSH)	1.10μL/mL	0.27-4.2
Calcitonin	<2.00 pg/mL	0-20

An analysis on histogram, mean, median and mode temperature, standard deviation, kurtosis and skewness per ROI and side is performed.

Results

Table 1 presents the statistical evaluation of mean, median, mode, standard deviation, kurtosis and skewness of the 2 defined bilateral ROIs during the whole images captured within the dynamic procedure. Figure 5 shows the thermal images taken from the dynamic procedure. It can be observed that the temperature dropped after cooling with the aluminum medals and started to recover immediately after, being the recover faster at the nodule affected ROI.

Figure 6 shows the evolution of the histograms over the 6 images taken during the examination, where it can be seenat none of the histograms followed the normal distribution.

Figure 7 presents the evolution for the 2 bilateral ROIs of the mean, median and mode temperature, standard deviation, kurtosis and skewness during the whole procedure. The mean, median, mode and standard deviation followed a similar pattern. The kurtosis provides a descriptor of the

shape of a probability distribution and showed a variability during the sequence of images, being higher at the nodule side. The skewness is a measure of the asymmetry of the probability distribution, also had some variability in the sequence of thermograms, being this variability different for both ROIs, the variations are subtler in non-nodule side and with an accentuated pattern at the nodule side.

The figure 8 shows the graph of the evolution of the thermal symmetry (Left ROI mean - Right ROI mean) during the sequence of IRT images, it can be observed that this value increases with the duration of the test, being higher than 0.8 ºC.

Table 2 shows the hormone values obtained from the blood tests of the subject, which are normal.

Discussion

This study has followed the IRT imaging guidelines (22-24) with respect to examination room and equipment preparation, the hypervascularized nodule was clear in the thermograms and more evident after cooling. The correlation of the findings in both imaging modalities is in line with the existing literature (11, 15). The mean, median, mode and thermal symmetry values are useful to discriminate the affected side from the contralateral normal side. The utility of the histograms and the value of skewness is debatable in discriminating the sites. No utility was found for the kurtosis value.

The use of histograms eases the task of identifying different data, the frequency of the data occurring in the ROI dataset and categories which are difficult to interpret in a tabular form, helping to visualize the distribution of the data within that ROI. This can be of extreme importance, as shown in this example (table 3), for understanding the thermal dynamic change of the data in small ROI.

All the numeric values obtained from the sequence of images along with rate of the change in temperature per pixels inside the ROI as suggested by the literature (21) in a large database of thyroid condition patients, may be used as inputs for machine learning classifiers (19, 20), which can be an important aid for physicians in their diagnosis of thyroid diseases.

The patient of this case study has to be regularly under surveillance due to the hypervascularization of the nodule found, despite the result of the blood tests for the thyroid hormones.

Conclusion

This case study showed evidence of the utility on using dynamic infrared thermal imaging when assessing thyroid nodules, which was confirmed by Doppler imaging to be highly vascularized and presenting a higher skin temperature when compared with the contralateral side. However, for diagnostic purposes, the traditional expensive methods such as biopsy and nuclear medicine are still required.

The application of IRT imaging should be further researched in monitoring and documenting the diagnosis and treatments evaluation applied to thyroid conditions such as cancer, hypothyroidism and hyperthyroidism. The application of image processing techniques along with the statistical evaluations of ROIs should be used to populate large databases and be inputs for decision support systems using artificial intelligence methods to aid physicians in their diagnosis.

Acknowledgements

Authors acknowledge the funding of projects LAETA - UID/EMS/50022/2013.

Conflict of Interest

The authors have no conflict of interest.

References

1. Guyton AC, Hall JE. Textbook of medical physiology. 11th ed. Pennsylvania: Elsevier Saunders, 2006.

2. Garcia M, Jemal A, Ward EM, Center MM, Hao Y, Siegel RL, Thun MJ. Global Cancer Facts & Figures 2008. Atlanta, GA: American Cancer Society, 2008.

3. Brown AP, Chen J, Hitchcock YJ, Szabo A, Schrieve DC, Tward JD. The risk of second primary malignancies up to three decades after the treatment of differentiated thyroid cancer. J Clin Endocrinol Metab, 2008, 93: 504-515.

4. Brown RL, de Souza JA, Cohen EE. Thyroid cancer: burden of illness and management of disease. J. Cancer, 2011, 2: 193-199.

5. Blankenship DR, Chin E, Terris DJ. Contemporary management of thyroid cancer. Am J Otolaryngol, 2005, 26: 249 -260

6. Manikantan K, Khode S, Dwivedi RC, Palav R, Nutting CM, Rhys-Evans P, Harrington KJ, Kazi R. Making sense of post-treatment surveillance in head and neck cancer: when and what of follow-up, Cancer Treatment Reviews, 2009, 35(8): 744-753.

7. Helmy A, Holdmann M, Rizkalla M. Application of Thermography for Non-Invasive Diagnosis of Thyroid Gland Disease. IEEE Trans. Biomed. Eng., 2008, 55: 1168-1175.

8. Karpman HA. Thermography in diagnosis of thyroid nodule. JAMA, 1971, 216(10): 1646-1647.

9. Samuels BI. Thermography: a valuable tool in the detection of thyroid disease. Radiology, 1972, 102(1): 59-62.

10. Galli G, Salvo D, Troncone L, De Rossi G. Combined thermography and isotope scanning in thyroid pathology. Acta Radiologica. Diagnosis, 1974, 15(6): 656-661.

11. Clark OH, Greenspan FS, Coggs GC, Goldman L. Evaluation of solitary cold thyroid nodules by echography and thermography. The American Journal of Surgery, 1975, 130(2): 206-211.

12. Di SP, Piva LUIGI, Viganotti G, Bertario LUCIO. Critical evaluation of the use of thermography in the investigation of scintigraphically cold thyroid nodules. Investigative radiology, 1982, 17(6): 607-609.

13. Aweda MA, Adeyomoye AO, Abe GA. Thermographic analysis of thyroid diseases at the Lagos university teaching hospital, Nigeria. Adv. Appl. Sci. Res, 2012, 3: 2027-2032.

14. Jin C, He ZZ, Yang Y, Liu J. MRI-based three-dimensional thermal physiological characterization of thyroid gland of human body. Medical engineering & physics, 2014, 36(1): 16-25.

15. Alves MLD, Gabarra MHC. Comparison of power Doppler and thermography for the selection of thyroid nodules in which fine-needle aspiration biopsy is indicated. Radiol Bras., 2016, 49(5): 311-315.

16. Jiang, L. J. et al. A perspective on medical infrared imaging. Journal of medical engineering & technology, 2005, 29(6): 257-267

17. Rossato M, Burei M, Vettor R. Neck thermography in the differentiation between diffuse toxic goiter during methimazole treatment and normal thyroid. Endocrine, 2015, 48(3): 1016-1017.

18. González JR, Rodrigues EO, Damião CP, Fontes CAP, Silva AC, Paiva AC, Li H, Du C, Conci A. An Approach for Thyroid Nodule Analysis Using Thermographic Images. Application of Infrared to Biomedical Sciences, 2017: 451-475.

19. González, JR, Damião C, Conci, A. An infrared thermal images database and a new technique for thyroid nodules analysis. In MEDINFO 2017: Precision Healthcare Through Informatics: Proceedings of the 16th World Congress on Medical and Health Informatics, IOS Press, 2018, 245: 384.

20. Bahramian F, Mojra A. Analysis of thyroid thermographic images for detection of thyroid tumor: An experimental?numerical study. Int J Numer Meth Biomed Eng, 2019: e3192.

21. Chan FHY, So ATP, Kung AWC, Lam FK, Yip HCL. Thyroid diagnosis by thermogram sequence analysis. Bio-medical materials and engineering, 1995, 5(3): 169-183.

22. Ring EFJ, Ammer K. Infrared thermal imaging in medicine. Physiological measurement 2012, 33(3): R33-R46.

23. Ring EFJ, Ammer K. The technique of infrared imaging in medicine, Thermology international 2000, 10(1): 7-14.

24. Ammer K. The Glamorgan Protocol for recording and evaluation of thermal images of the human body, Thermology international 2008, 18(4): 125-144.

Address for Correspondence:

Ricardo Vardasca, Ph.D., ASIS, FRPS
Faculdade de Engenharia, Universidade do Porto,
Rua Dr. Roberto Frias S/N, 4200-465 Porto, Portugal

Email: ricardo.vardasca@fe.up.pt

(Received 07.10.2019, revision accepted 28.10.2019)

Wroclaw announced as host city for XV Congress of the European Association of Thermology, 1st - 4th September 2021

Maria Soroko

Department of Horse Breeding and Equestrian Studies, Wroclaw University of Environmental and Life Sciences, Wroclaw, Poland
Local organising committee chair, XV Congress of the European Association of Thermology, Wroclaw

The European Association of Thermology is delighted to announce that the XV Congress of the EAT will take place 1st - 4th September 2021 in the beautiful city of Wroclaw in Poland. This sees the EAT Congress return to eastern Europe after our recent very successful visits to Portugal (2012), Spain (2015) and London (2018).

Our venue will be the Faculty of Biology and Animal Science at the prestigious Wroclaw University of Environmental and Life Sciences, where longstanding EAT member Dr. Maria Soroko is a Research Associate and Lecturer.

About the city

Wroclaw lies on the banks of the River Oder in western Poland, and is the capital of the Lower Silesian Vovoideship. It was the European Capital of Culture in 2016, and won the "European Best Destination" title in 2018.

Notable landmarks include the 10th century Cathedral, the Centennial Hall from 1913 (registered as a UNESCO World Heritage Site), and the distinctive architecture of the Town Hall and Market Square. Wroclaw is also host to the Raclawice Panorama, a 114m-long cycloramic painting from 1894, commemorating the 100th anniversary of the Battle of Raclawice.

In recent years Wroclaw has also become well-known for its "little people" or "dwarves": small figurines scattered across the city streets which were first conceived as part of the city's anti-communist movement in 2005. These now

number more than 350, and can be located with the help of a dedicated tourist map.

Wroclaw Zoo, close to our congress venue, is the oldest zoo in Poland, and the third largest zoological gardens in the world in terms of the number of species on display.

In summertime, large numbers of visitors are attracted at night to Wroclaw's "Multimedia Fountain" close to the Centennial Hall. This is one of the largest operating fountains in Europe, and stages dramatic light shows set to music. We will have the opportunity to visit this spectacle as part of the congress social programme.

Wroclaw has excellent road and rail transport connections, and is served by Copernicus Airport, situated just 10km from the city centre.

About the congress venue

Wroclaw University of Environmental and Life Sciences has its origins in the University of Breslau Institute of Agriculture, which opened on Mattiaplatz in 1881. The Institute moved to Hansastrasse in 1923, which remains the main building of the university to this day. Higher education in Wroclaw was entirely restructured in 1945 to form the State University and Polytechnic. After 1951, the School of Agriculture was separated from these establishments to become a distinct university, finally adopting its current title in 2006. The university is currently the place of education for around 13,000 students.

Our congress venue is the Faculty of Biology and Animal Science on Chelmonskiego in the eastern suburbs of Wroclaw. The Faculty building boasts excellent conference facilities including a large lecture theatre, ample lobby space for networking and poster presentations, and a spacious restaurant for lunch breaks. This is the perfect environment for delegates to present their thermological research at Europe's flagship biomedical temperature congress.

A formal "first announcement" with further information will be distributed in January 2020. The congress "Call for Abstracts" will be published in July, with abstract submission closing on 31st December 2020.

It will be our pleasure to welcome you to the XV Congress of the EAT and Poland's best-kept secret: historic Wroclaw! Save the date - and see you all in September 2021!

2020

17th-19th April 2019

24th Conference of the Polish Association of Thermology Combined with the European Association of Thermology in Zakopane

Conference venue:
HYRNI Hotel, Pilsudskiego str 20, Zakopane

Abstract deadline March 15th 2019
Please send your abstract to
a.jung@spencer.com.pl or
armand.cholewka@gmail.com

Accepted abstracts will be published in Thermology International.

Accommodation (2 nights) / meals, welcome dinner 130 E per person (participant, accompanying person) will be paid in cash/credit card on arrival in hotel reception

EARLY RESERVATION FOR ACCOMMODATION before March 15th to ensure hotel reservation by email to a.jung@spencer.com.pl

Organising Committee

Prof.Armand Cholewka Ph.D, Eng

Prof.Anna Jung MD, Ph.D

Dr.Janusz Zuber MD,Ph,D

Teresa Kasprzyk MSc,Eng

Dr.Anna Kowalczyk MD,Ph.D

Scientific Committee

Dr.Kevin Howell Ph.D (UK)

Prof.Kurt Ammer MD,Ph.D (AUT)

Prof.Sillero-Quintana Manuel Ph.D (SPA)

Aderito Seixas Msc, DPT, (POR)

Dr.Ricardo Vardasca Ph.D (POR)

Prof.Armand Cholewka Ph.D,Eng (Poland)

Prof.Anna Jung MD,Ph.D (Poland)

Prof.Antoni Nowakowski Ph.D, Eng (Poland)

Dr.Janusz Zuber MD,Ph.D (Poland)

Prof.Boguslaw Wiecek Ph.D, Eng (Poland)

PROGRAMME AT A GLANCE.

17th April, Friday - 7 p.m.
Welcome Dinner (HYRNY Hotel)

18th April, Saturday

9.00 - 11.00 Session I

11.00 - 11.20 Coffee break

11.20 -13.00 Session II

13.00 - 14.15 Lunch

14.30 - 16.00 Session III

16.00 - 16.15 Coffee break

16.15 - 18.00 EAT board meeting

Further information:

Prof Anna Jung
a.jung@spencer.com.pl or
Prof. Armand Cholewka
armand.cholewka@gmail.com

6th - 10th July 2020

The 15th Conference on Quantitative InfraRed Thermography in Porto, Portugal

For further information and updates, please visit the website: **http://www.qirt2020.com** or

contact the organizing committee at
qirt2020@fe.up.pt

See pages 157 and 158

Call for Papers

Since 1992, the Quantitative InfraRed Thermography (QIRT) conference is a biannual international forum which brings together specialists from industry and academia, who share an active interest in the latest developments of science, experimental practices and instrumentation, related to IR thermography.

Following conferences in Paris (1992), Sorrento (1994), Stuttgart (1996), Lodz (1998), Reims (2000), Dubrovnik (2002), Brussels (2004), Padova (2006), Krakow (2008), Québec City (2010) and Naples (2012), Bordeaux (2014), Gdansk (2016) and Berlin (2018), QIRT 2020 will take place in Porto, Portugal. Since 2015, due to the growing QIRT community, a sister conference series, QIRT-Asia, was established. Chennai (India) 2015, Daejon (Korea) 2017 and Tokyo (Japan) 2019. All conference proceedings are available through the QIRT Conference Open Archives at www.qirt.org.

QIRT 2020 will cover, but will not be limited to, the following topics:

- State of the art and evolution in the field of IR scanners and imaging systems allowing quantitative measurements and related data acquisition and processing.
- Integration of thermographic systems and multispectral analysis. Related problems like: calibration and characterization of IR cameras, emissivity determination, absorption in media, spurious radiations, 3D measurements, certification and standardization.
- Thermal effects induced e.g. by electromagnetic fields, elastic waves or mechanical stresses.
- Application of IR thermography to radiometry, thermometry and physical parameters identification in all fields such as: industrial processes, material sciences, thermo-fluid dynamics, energetics, non-destructive evaluation, cultural heritage, environment, medicine, biomedical science, food production…

Important dates

- **Abstract submission deadline: November 30, 2019**
- **Acceptance notification: February 29, 2020**
- **Paper submission deadline: April 30, 2020**

Abstract and Paper Submission

The participants are invited to submit to the QIRT 2020 Web Site (http://www.qirt2020.com) by November 30, 2019 an **extended abstract** of 2 pages (a template is provided at the website), either for oral or poster presentation, including key figures and main results. A book of abstracts will be distributed at the conference.

Following acceptance notification, **camera ready, full paper** of 6-10 pages including colour figures should be submitted to the QIRT 2020 web site by April 30th, 2020.

All submissions for oral or poster presentation will be handled electronically via the conference website **http://www.qirt2020.com**

A Word template to be used for both abstracts and full papers is downloadable at the website.

Authors are requested to propose the thematic section in which the paper should be included.

Web-Based Proceedings and possible publication in QIRT Journal

Presented papers (oral and posters) will be published online in the QIRT Open-Archives, which can be found at the website: **www.qirt.org**. A USB flash drive with all conference papers will be also distributed to the conference participants.

After the conference, the Scientific Committee will carry out a pre-selection of the most prominent presented papers for a possible publication in Quantitative InfraRed Thermography Journal after a subsequent review by two experts.

Steering Committee

X. Maldague (Canada) *Chairman*
P. Bison (Italy)
J. Dumoulin (France)
D. Balageas (France)
J.C. Batsale (France)
G. Busse (Germany)
C. Maierhofer (Germany)
J.M. Buchlin (Belgium)
G. Cardone (Italy)
G.M. Carlomagno (Italy)
A. Nowakowski (Poland)
A. Salazar (Spain)
S. Svaic (Croatia)
B. Wiecek (Poland)
V. Vavilov (Russia)
J. Morikawa (Japan)
Won Tae Kim (Korea)

International Scientific Committee

D. Balageas (France)
J.C. Batsale (France)
C. Bissieux (France)
J.M. Buchlin (Belgium)
G. Busse (Germany)
G. Cardone (Italy)
G.M. Carlomagno (Italy)
E. Cramer (U.S.A.)
B. Jähne (Germany)
P. Lybaert (Belgium)
C. Maierhofer (Germany)
X. Maldague (Canada)
P. Millan (France)
A. Nowakowski (Poland)
B. Oswald-Tranta (Austria)
A. Rozlosnik (Argentina)
A. Salazar (Spain)
T. Schrijer (The Nederlands)
S. Shepard (USA)
S. Svaic (Croatia)
B. Wiecek (Poland)
H. Wiggenhauser (Germany)
V. Vavilov (Russia)

Organizing Committee

J. Mendes *(chairman)*
R. Vardasca *(chairman)*
R. Natal Jorge
J. Tavares
M. Clemente
A. Seixas
C. Magalhaes

Pre-Conference short courses

QIRT short courses

In addition to the main technical program, the conference will include one-day short courses (Monday, July 6).

It will include:

- Non-destructive testing using active thermography
- Non-destructive testing using lock-in thermography
- Passive and active thermography in civil engineering
- Thermal problems in fluid dynamics
- Analytical solutions for passive and active thermography
- Biomedical thermography applications.

The fee to attend the short course will be 200 € (VAT, coffee breaks and lunch included).

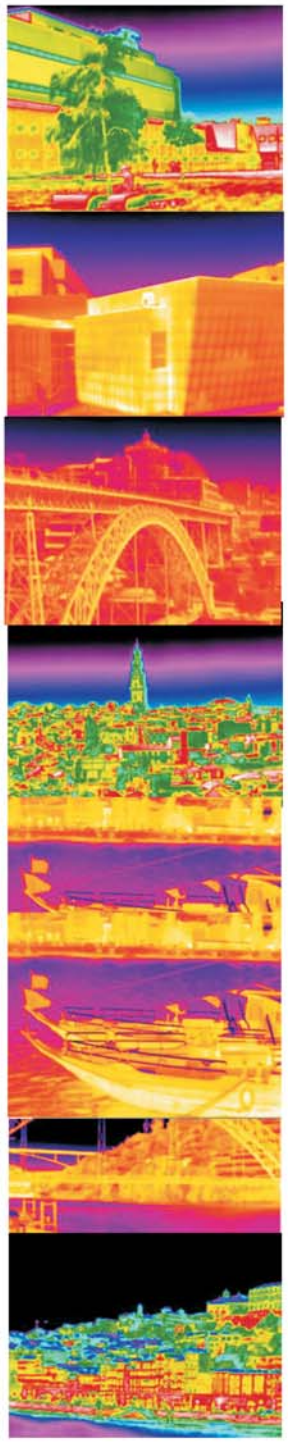

Awards

During the conference, the best scientific paper will be honoured by the Grinzato Award and the best student paper by the Student Award.

Application for the Student Award is indicated at abstract submission. The nominees for the Grinzato Award will be announced by the steering committee according to the rating of the submitted abstracts.

Conference fees (VAT included)

Regular participants

- Early rate (deadline: May 30, 2020): 700 €
- Late rate (deadline: June 30, 2020): 750 €
- Desk registration rate: 800 €

Students & over 66<

- Early rate (deadline: May 30, 2020): 350 €
- Late rate (deadline: June 30, 2020): 400 €
- Desk registration rate: 450 €

Fee covers: Book of abstracts, Conference USB Proceedings, Welcome reception, Conference dinner, 4 lunches and coffee breaks. Accommodation is not included.
For regular participants only, **fee includes also a subscription to QIRT Journal for 2 years** (Standard personal subscription rate).

Accompanying persons

- Rate (deadline: June 30, 2020): 160 €

This amount includes the Porto visiting card (with free transport for 4 days and discounts in touristic places), Welcome reception and Conference dinner.

Venue

QIRT 2020 will be held at the Faculty of Engineering, University of Porto. The city of Porto has been recognized as the best European destination in 2014 and 2017.

A list of hotels will be given in the conference website. Booking of hotel is not assumed by the conference organization.

Host organization

Faculty of Engineering, University of Porto, Portugal

For further information and updates, please visit the website: **http://www.qirt2020.com** or contact the organizing committee at **qirt2020@fe.up.pt**

The Thermal Human Body

A Practical Guide to Thermal Imaging

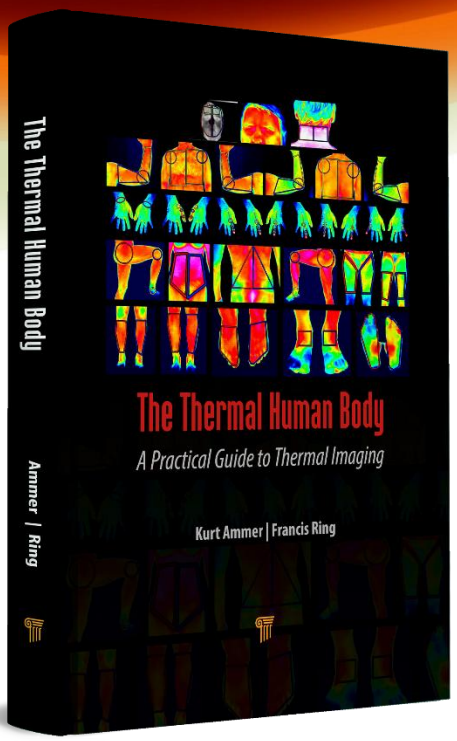

by
Kurt Ammer & Francis Ring

978-981-4745-82-6 (Hardback)
978-0-429-01998-2 (eBook)
US$149.95
260 Pages – 19 Color & 38 B/W Illustrations
May 2019

Key Features

- Combines the physics of heat transfer with thermal physiology to understand skin temperature distribution
- Provides a framework for standardized recording and analysis of medical thermal images
- Includes an atlas of body positions of proven reproducibility for infrared image capture
- Proposes regions of interests for reliable quantitative analysis

How to Order

SAVE 20% with FREE standard shipping when you order online at **www.crcpress.com** and enter Promo Code **PAN01.**
Alternatively, you can contact your nearest bookstore, or our distributor as follows:

CRC Press (*Taylor & Francis*)
6000 Broken Sound Parkway NW, Suite 300
Boca Raton, FL 33487, USA
Tel: +1 800-272-7737
Fax: +1 800-374-3401
Email: **orders@taylorandfrancis.com**

Reviews

"There is no way to study thermal imaging and not learn from the writings of Francis Ring and Kurt Ammer. Pioneers of the application of infrared thermography in medicine, the authors unveil the direction for a sensible use of the method. Luck for us—students, professionals and enthusiasts—because we can be grateful to receive a differentiated material that shortens the learning path. No doubt a remarkable book."
- **Prof. Danilo Gomes Moreira**, Science and Technology of Minas Gerais, Brazil

"This book is set to become essential reading for anyone who wants to perform reliable thermal imaging of the human body, whether it be in medicine, clinical practice, sports science or research."
- **Prof. Graham Machin**, National Physical Laboratory, UK

"This book is a wonderful practical guide that takes the reader through all the main stages required and will be of special interest for those interested in entering the fascinating field of clinical thermal imaging."
- **Prof. James B. Mercer**, UiT—The Arctic University of Norway, Norway

Description

This book is a guide for the constantly growing community of the users of medical thermal imaging. It describes where and how an infrared equipment can be used in a strictly standardized way and how one can ultimately comprehensively report the findings. Due to their insight into the complex mechanisms behind the distribution of surface temperature, future users of medical thermal imaging should be able to provide careful, and cautious, interpretations of infrared thermograms, thus avoiding the pitfalls of the past. The authors are well-known pioneers of the technique of infrared imaging in medicine who have combined strict standard-based evaluation of medical thermal images with their expertise in clinical medicine and related fields of health management.

JENNY STANFORD PUBLISHING